Chemical Vapor Deposition and Functionalization of Fluorocarbon-Organosilicon Copolymer Thin Films

by

Shashi Krishna Murthy

B.S. Chemical Engineering
The Johns Hopkins University, 1999

Submitted to the Department of Materials Science and Engineering
in Partial Fulfillment of the Requirements for the Degree of

DOCTOR OF PHILOSOPHY IN POLYMER SCIENCE
AT THE
MASSACHUSETTS INSTITUTE OF TECHNOLOGY

June 2003

© 2003 Massachusetts Institute of Technology. All rights Reserved.

Signature of Author ....
Department of Materials Science and Engineering
May 2, 2003

Certified by ....
Karen K. Gleason
Professor of Chemical Engineering
Thesis Supervisor

Accepted by ....
Harry L. Tuller
Professor of Ceramics and Electronic Materials
Chair, Departmental Committee on Graduate Students

Chemical Vapor Deposition and Functionalization of Fluorocarbon-Organosilicon Copolymer Thin Films

by

Shashi Krishna Murthy

Submitted to the Department of Materials Science and Engineering
on May 2, 2003 in Partial Fulfillment of the Requirements for the Degree of
Doctor of Philosophy in Polymer Science

ABSTRACT

Neural prostheses are micron-scale integrated circuit devices that are under development for the treatment of brain and spinal cord injuries. A key challenge in the fabrication of these silicon-based devices is the protection of the electronic components from the ambient body environment. There is a need for a biopassivation coating on these devices that is chemically inert and electrically insulating with good adhesion to the underlying silicon substrate. Fluorocarbon-organosilicon copolymers are of interest for this application because they have the desirable attributes of both fluorocarbon and organosilicon polymers, such as low dielectric constant, thermal stability, and good adhesion to silicon. Chemical vapor deposition (CVD) is an attractive synthetic technique for this application because it is single-step, requires no solvent, and allows conformal coatings to be deposited on substrates with complex topographies and small dimensions.

Fluorocarbon-organosilicon copolymers have been synthesized by hot-filament CVD, a thermal CVD technique. Control over deposition rate and chemical structure is achieved by precursor choice and variation of filament temperature. Chemical characterization by infrared (FTIR), x-ray photoelectron (XPS), and solid-state nuclear magnetic resonance (NMR) spectroscopies indicates that the copolymer films range from highly cross-linked films to flexible films comprised mostly of linear polymer chains. This variation in chemical composition influences physical properties such as thermal stability and flexibility. The possibility of creating bioactive surface coatings has been explored by using the techniques of CVD and solution chemistry in combination. Chains of poly(acrylamide) have been grafted onto fluorocarbon-organosilicon films as a first step towards the design of bioactive coatings that could potentially enhance the performance of medical implants.

Thesis Supervisor: Karen K. Gleason
Title: Professor of Chemical Engineering

Acknowledgments

The completion of this thesis represents the culmination of four eventful and fruitful years of my life. A number of things came together in perfect harmony over these years, thanks to the efforts of many.

I thank my advisor, Prof. Karen Gleason, for being a wonderful mentor. Your patient guidance and constant support have been valuable to me over the last four years. Your pragmatic approach in identifying and solving problems and developing new ideas has taught me a great deal. I am grateful to the members of my thesis committee, Profs. Michael Rubner and Caroline Ross, for being very supportive and appreciative of my work. I would also like to thank Dr. David Edell for his guidance on work done in the area of biopassivation coatings.

My years at MIT would have been very different and considerably more difficult had it not been for the assistance of my UROP student, Brad Olsen. Students of your intellect and ability are rare, even at an institution like MIT. I consider it a privilege to have had the opportunity to work with you and am deeply grateful for the contributions that you have made to this thesis. The experience of working with you has contributed immensely to my intellectual growth. I hope that I have been able to teach you a few things in return.

Many thanks are due to the past and present members of the Gleason group. I am especially grateful to Ken Lau, who has been a mentor since my very first days in the group and a good friend. A special nod goes to Dan Burkey, whose lively personality and witty repartee gave color to life in the windowless 66-419 office.

I am grateful to Prof. Rubner for encouraging me to join the PPST program during my visit to MIT as a prospective graduate student in the spring of 1999. I also acknowledge the support and guidance provided by Prof. Rubner to me and other members of my PPST class during our first year as we navigated our way through the core curriculum and qualifying exams. Special thanks are due to Prof. Sam Allen for being an invaluable source of advice on academic careers.

I am grateful to the folks in the DMSE administration, in particular Gloria Landahl, Angelita Mireles, Kathy Farrell, Ken Greene, Steve Malley, and Jenna Picceri who have always been there to answer my questions with a smile and help me out with matters big and small.

Table of Contents

Abstract 2

Acknowledgments 3

List of Figures 6

List of Tables 9

List of Notations and Abbreviations 11

CHAPTER ONE 12

Introduction

1.1 Motivation 13
1.2 Chemical Vapor Deposition 14
1.3 Fluorocarbon Polymers 16
1.4 Organosilicon Polymers 19
1.5 Fluorocarbon-Organosilicon Copolymers 21
1.6 Thesis Framework 23
1.7 References 24

CHAPTER TWO 26

Fluorocarbon-Organosilicon Copolymer Synthesis by Hot Filament Chemical Vapor Deposition

Abstract 27
2.1 Introduction 28
2.2 Experimental Section 30
2.3 Results and Discussion 32
2.4 Conclusions 44
2.5 References 44

CHAPTER THREE 47

Initiation of Cyclic Vinylmethylsiloxane Polymerization in a Hot-Filament Chemical Vapor Deposition Process

Abstract 48
3.1 Introduction 49
3.2 Experimental Section 50
3.3 Results and Discussion 52
3.4 Conclusions 62
3.5 References 63

CHAPTER FOUR 65

Effect of Filament Temperature on the Chemical Vapor Deposition of Fluorocarbon-Organosilicon Copolymers

Abstract 66
4.1 Introduction 67
4.2 Experimental Section 68
4.3 Results and Discussion 70
4.4 Conclusions 90
4.5 References 90

CHAPTER FIVE 93

Graft Functionalization of Fluorocarbon-Organosilicon Copolymer Thin Films

Abstract 94
5.1 Introduction 95
5.2 Experimental Section 97
5.3 Results and Discussion 100
5.4 Conclusions 106
5.5 References 107

CHAPTER SIX 109

Summary and Suggestions for Future Work

6.1 Summary 110
6.2 Suggestions for Future Work 112
6.3 References 114

APPENDIX 115

Adhesion and Electrical Properties of Fluorocarbon-Organosilicon Copolymer Films

A.1 Introduction 116
A.2 Experimental Section 116
A.3 Results and Discussion 119
A.4 Conclusions 122
A.5 References 122

List of Figures

CHAPTER ONE

Figure 1.1 Problems encountered in the operation of implantable integrated circuits.

Figure 1.2 Comparison of continuous PECVD (top) and pulsed PECVD (bottom) coating of 75 μm diameter wires. In the pulsed PECVD case, the crosslinking density has been reduced below the percolation of rigidity, allowing the structural integrity of the coating to be maintained even after tying the wires into 800 μm diameter loops.

Figure 1.3 Cross-sectional view of a CVD fluorocarbon coated silicon microribbon. (a) Full view with scale bar = 20 μm. (b) Corner magnification with scale bar = 10 μm.

Figure 1.4 Environmental scanning electron micrograph of Iridium neural probe with a 9 mm PECVD fluorocarbon coating.

Figure 1.5 Pulsed plasma enhanced CVD organosilicon coated silicon microribbon cable.

Figure 1.6 Pulsed plasma enhanced CVD organosilicon coated UM neural probe.

CHAPTER TWO

Figure 2.1 FTIR spectra of (a) copolymer, (b) silicone, and (c) fluorocarbon films, all deposited by HFCVD under the same conditions.

Figure 2.2 Low-wavenumber region from the FTIR spectrum of the copolymer film.

Figure 2.3 Carbon (1s) high-resolution scan of the HFCVD copolymer film showing CF_2 and CH_3 peaks.

Figure 2.4 Solid-state ^{19}F NMR spectrum of the HFCVD copolymer film. The feature at –72 ppm is a spectrometer artifact.

Figure 2.5 Solid-state ^{13}C NMR spectra of the HFCVD copolymer film obtained with (a) ^{1}H and (b) ^{19}F decoupling.

Figure 2.6 Solid-state ^{29}Si NMR spectra of the HFCVD copolymer film obtained with (a) ^{1}H and (b) ^{19}F cross-polarization and decoupling.

CHAPTER THREE

Figure 3.1 Deposition rates of HFCVD films deposited from V_3D_3 and PFOSF as a function of filament temperature (T_f). Data points marked with circles are for films deposited

from V_3D_3 and PFOSF. The data point marked with a square represents a film deposited from V_3D_3 alone.

Figure 3.2 Solid-state ^{19}F NMR spectrum of the HFCVD film deposited at a filament temperature of 370 °C. The feature at –72 ppm is a spectrometer artifact.

Figure 3.3 Solid-state ^{13}C NMR spectra of the HFCVD film deposited at a filament temperature of 370 °C obtained with (a) ^{19}F decoupling and (b) ^{1}H decoupling.

Figure 3.4 FTIR spectrum of the film deposited at a filament temperature of 370°C.

CHAPTER FOUR

Figure 4.1 ^{13}C NMR spectra of the HFCVD films deposited at filament temperatures of (a) 370 °C, (b) 440 °C, and (c) 540 °C. Spectra were obtained by direct polarization with proton decoupling.

Figure 4.2 ^{29}Si NMR spectra of the HFCVD films deposited at filament temperatures of (a) 370 °C, (b) 440 °C, and (c) 540 °C. Spectra were obtained with proton cross-polarization and proton decoupling.

Figure 4.3 FTIR spectra of the films deposited at filament temperatures of (a) 370 °C, (b) 440 °C, and (c) 540 °C.

Figure 4.4 Expanded FTIR spectra of the films deposited at filament temperatures of (a) 370 °C, (b) 440 °C, and (c) 540 °C showing the region of the CH_3 symmetric bending mode in Si-CH_3 groups.

Figure 4.5 TGA results of the HFCVD films deposited at three different filament temperatures.

Figure 4.6 Environmental scanning electron micrographs of fluorocarbon-organosilicon copolymer wire coatings on 50 μm diameter platinum wires deposited using filament temperatures of (a) 370 °C, (b) 440 °C, and (c) 540 °C.

CHAPTER FIVE

Figure 5.1 Carbon (1s) high-resolution scan of the fluorocarbon-organosilicon copolymer film before and after PAM grafting. Peak assignments are taken from refs. 21 and 22. the presence of PAM on the surface is evidenced by the presence of the carbonyl group peak.

Figure 5.2 Atomic force micrographs of a fluorocarbon-organosilicon film deposited on a silicon wafer (a) before and (b) after PAM grafting. The image area for both micrographs is 500 nm^2, and the vertical scale is 35 nm/division.

APPENDIX

Figure A.1 Schematic diagram of soak test assembly.

Figure A.2 Optical micrographs of a fluorocarbon-organosilicon copolymer film before (left) and after (right) saline soak testing. The surface of the film is covered with particles that appear to suffer corrosion upon immersion in saline.

List of Tables

CHAPTER TWO

Table 2.1 Absorption band assignments for FTIR spectra.

Table 2.2 XPS survey scan data.

Table 2.3 Chemical shift assignments for the ^{19}F NMR spectrum.

Table 2.4 Chemical shift assignments for the ^{13}C NMR spectra.

Table 2.5 Chemical shift assignments for the ^{29}Si NMR spectra.

CHAPTER THREE

Table 3.1 Chemical shift assignments for the ^{19}F spectrum.

Table 3.2 Chemical shift assignments for the ^{13}C NMR spectra.

Table 3.3 Absorption band assignments for FTIR spectrum.

CHAPTER FOUR

Table 4.1 Chemical shift assignments for the ^{13}C NMR spectra of Figure 4.1.

Table 4.2 Chemical shift assignments for the ^{29}Si NMR spectra of Figure 4.2.

Table 4.3 Absorption band assignments for FTIR spectra of Figure 4.3.

Table 4.4 FTIR peak fit areas and vinyl group loss quantification.

Table 4.5 Percolation of rigidity calculations for the HFCVD film deposited with a filament temperature of 370 °C.

Table 4.6 Percolation of rigidity calculations for the HFCVD film deposited with a filament temperature of 440 °C.

Table 4.7 Percolation of rigidity calculations for the HFCVD film deposited with a filament temperature of 540 °C.

CHAPTER FIVE

Table 5.1 XPS survey scan data.

Table 5.2 Water contact angles on fluorocarbon-organosilicon copolymer film before and after PAM grafting.

APPENDIX

Table A.1 Adhesion test results for HFCVD films.

Table A.2 Resistivity measurements from saline soak tests.

List of Notations and Abbreviations

AFM	atomic force microscopy
ASM	asymmetric stretching mode
CF_4	tetrafluoromethane
C_6F_6	perfluorobenzene
CP	cross-polarization
CVD	chemical vapor deposition
D_3	hexamethylcyclotrisiloxane
DD	dipolar decoupling
ESEM	environmental scanning electron microscopy
FTIR	Fourier transform infrared spectroscopy
H_4D_4	1,3,5,7-tetramethylcyclotetrasiloxane
HFCVD	hot-filament chemical vapor deposition
HFPO	hexafluoropropylene oxide
HMDSO	hexamethyldisiloxane
MAS	magic angle spinning
MFC	mass flow controller
NMR	nuclear magnetic resonance
PAM	poly(acrylamide)
PDMS	poly(dimethylsiloxane)
PECVD	plasma-enhanced chemical vapor deposition
PFOSF	perfluorooctane sulfonyl fluoride
PTFE	poly(tetrafluoroethylene)
$<r>$	average connectivity number
RF	radio frequency
TGA	thermogravimetric analysis
UV	ultraviolet
V_3D_3	1,3,5-trivinyl-1,3,5-trimethylcyclotrisiloxane
V_4D_4	1,3,5,7-tetravinyl-1,3,5,7-tetramethylcyclotetrasiloxane
VIS	visible
XPS	x-ray photoelectron spectroscopy

Chapter One

Introduction

1.1 Motivation

An important milestone in the treatment of neurological disorders (such as stroke, paralysis, and Parkinson's disease) has been the development of implantable integrated circuit devices.[1] These devices are typically silicon-based integrated circuits that are designed to send and receive electrical signals to and from neurons in the central nervous system. The devices can be used to stimulate areas of the brain and spinal cord to restore functions of the body that are lost due to injury or disease. A key challenge in the fabrication of these prosthetic devices is the protection of the integrated circuitry from the ambient body environment. Figure 1.1 illustrates some of the problems encountered in the operation of these devices.

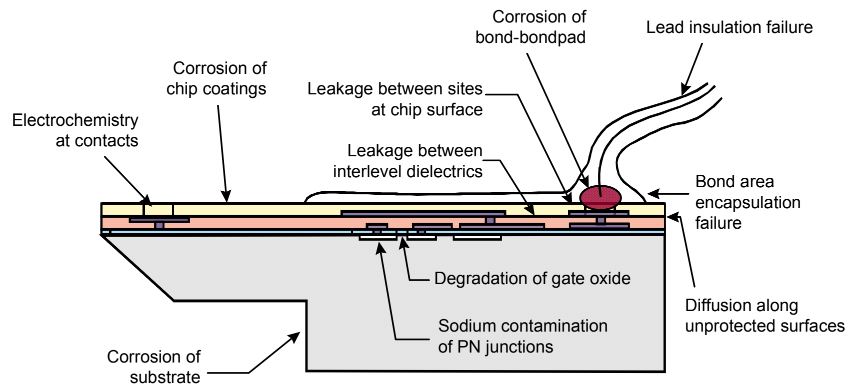

Figure 1.1 Problems encountered in the operation of implantable integrated circuits.

The electronic components of these devices therefore need to be protected with a biopassivation coating that adheres well to the underlying silicon substrate, and is also electrically insulating, chemically inert, non-permeable, and thermally stable at the temperature of assembly of the device (~ 150 °C). Furthermore, since neural prostheses have complex topographies and micron-scale dimensions, it is important to have coatings that are

extremely thin, in order to minimize tissue damage.[2] An additional requirement is that the technique used to apply the coating be compatible with the vacuum-based methods of integrated circuit fabrication.

1.2 Chemical Vapor Deposition

The use of conventional gel or liquid coating techniques to apply biopassivation coatings onto neural prostheses is undesirable because surface tension and capillary effects can damage the fine, micron-scale features on the devices. In addition, thin, conformal coatings cannot be made reproducibly. Chemical vapor deposition (CVD) is a technique by which thin, conformal coatings can be synthesized and applied onto substrates with complex topographies and small overall dimensions. This method is particularly attractive for neuroprosthetic applications because it is compatible with integrated circuit manufacturing processes.

Two CVD techniques of interest for this application are plasma-enhanced CVD and hot-filament CVD. Plasma-enhanced CVD (PECVD) is a technique that involves the generation of a low-density plasma by radio frequency (RF) excitation of a precursor gas at low pressure (< 10 Torr). The plasma consists of ions, radicals, and excited neutrals, which can undergo reactions to form a thin film on the surface of a substrate.

A variety of problems have limited the applicability of PECVD films for biopassivation applications. The most significant of these are the high dielectric loss of these films (when compared to conventional polymers), and aging effects upon exposure to the atmosphere.[3] Both of these effects can be related to the high density of trapped radicals in

plasma-deposited materials, so-called “dangling bond” defects. When exposed to the atmosphere, these dangling bonds are oxidized, leading to concomitant changes in film structure and properties. Dangling bond defects can originate from electron impact fragmentation of gaseous reactants, UV irradiation,[4] and/or ion bombardment of the surface.[5] Plasma exposure of the surface also increases the crosslinking density of the film. Although some crosslinking is desired, an extremely high degree of crosslinking can result in brittle and inflexible films.

These shortcomings can be limited by pulsing the plasma excitation on a millisecond time scale. When the RF power is on, both ions and reactive neutrals are produced in the gas phase. However, ions often have much shorter lifetimes than neutrals. Hence when the RF power is turned off, the ratio of neutrals to ions will increase and film deposition from reactive neutrals will be favored. Also, the decrease in ion bombardment leads to a reduction in the number of dangling bonds and the degree of crosslinking in the growing film.[6-8]

In hot-filament CVD (HFCVD), a precursor gas is thermally decomposed by a resistively heated filament. The resulting pyrolysis products adsorb onto a substrate maintained at room temperature and react to form a film. This method does not involve ion bombardment or UV irradiation, and has been shown to provide films with a substantially lower density of dangling bonds and crosslinking.[9] Films produced by this method can be characterized more easily because there are fewer reaction pathways available than in the less-selective PECVD process. The temperature range required for pyrolysis depends on the identity of the precursor gas selected.

1.3 Fluorocarbon Polymers

Fluorocarbon polymers are well known for having highly desirable properties for biomedical applications. These properties include chemical stability, electrical insulation, and biocompatibility. One such polymer, poly(tetrafluoroethylene) (PTFE, also known as Telfon®), has been used widely as a biomaterial. Application areas include vascular grafts, heart valve components, sutures, and tissue reconstruction, to name only a few. Extensive work has been done on the vapor deposition of fluorocarbon thin films. A comprehensive review of work in this area has been written by d'Agostino et al.[10] The use of plasma-polymerized fluorocarbons as biomaterials has been discussed by Gombotz and Hoffman.[11]

Limb et al[7] developed a method to deposit fluorocarbon films spectroscopically similar to PTFE using PECVD. The precursor used in this process was hexafluoropropylene oxide (HFPO). It was demonstrated that the chemical composition and physical properties could be tuned by pulsing the plasma excitation, as shown in Figure 1.2.[7]

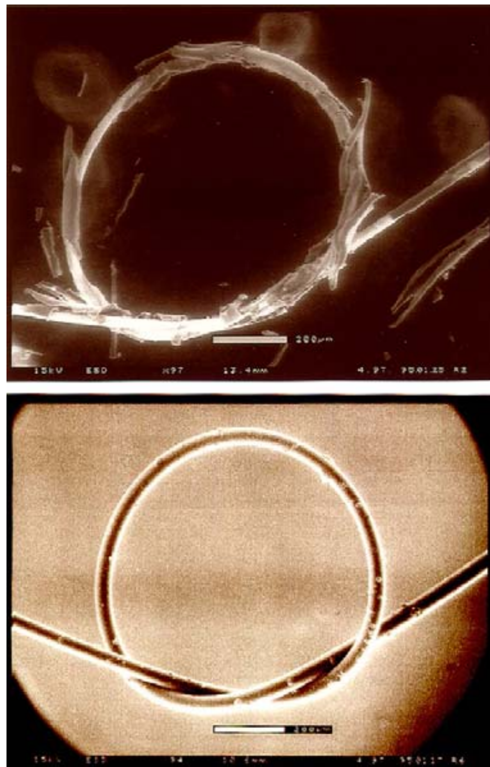

Figure 1.2 Comparison of continuous PECVD (top) and pulsed PECVD (bottom) coating of 75 μm diameter wires. In the pulsed PECVD case, the crosslinking density has been reduced below the percolation of rigidity, allowing the structural integrity of the coating to be maintained even after tying the wires into 800 μm diameter loops.[7]

Limb et al also used the PECVD technique to produce fluorocarbon coatings on components of neurological electrode assemblies, such as silicon microribbons and neural probes. Cross-sectional views of a coated microribbon are shown in Figure 1.3. Figure 1.4 shows a Huntington Medical Research Institute (HMRI) probe coated with a fluorocarbon film. The coating produced by PECVD is uniform up to the tip (which is 5 μm in diameter). Figures 1.3 and 1.4 demonstrate the ability to create conformal coatings on micron-scale components of neural prostheses using CVD.

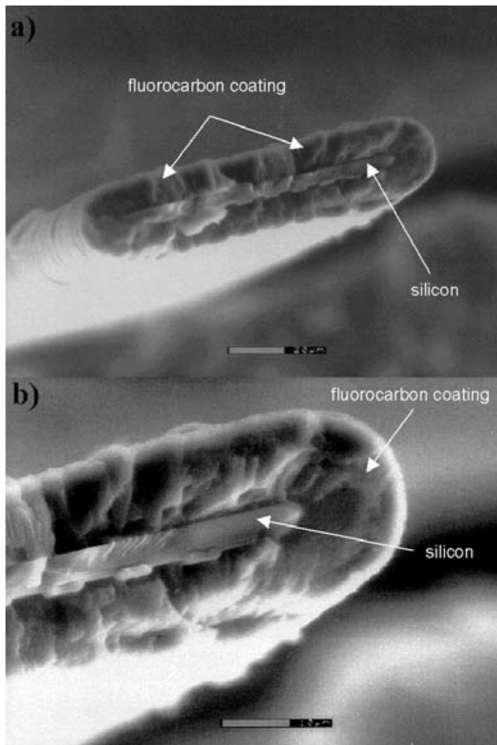

Figure 1.3 Cross-sectional view of a CVD fluorocarbon coated silicon microribbon. (a) Full view with scale bar = 20 μm. (b) Corner magnification with scale bar = 10 μm.

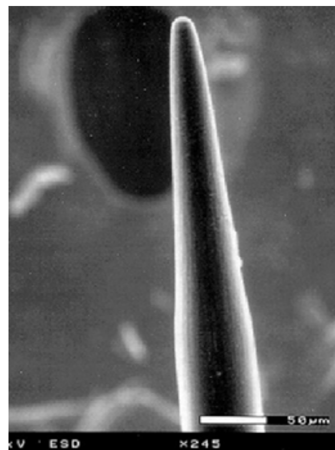

Figure 1.4 Environmental scanning electron micrograph of Iridium neural probe with a 9 μm PECVD fluorocarbon coating.[7]

1.4 Organosilicon Polymers

The use of organosilicon films prepared by CVD techniques as biomaterials has been investigated by several researchers. Organosilicon coatings on Celgard®-2400 and Silastic® membranes were deposited from two cyclic silicone precursors (hexamethylcyclotrisiloxane and octamethylcyclotetrasiloxane) using PECVD by Chawla.[12] The adhesion of platelets and leucocytes to the coated membranes was found to be lower than adhesion on untreated controls. Ishikawa et al[13] obtained similar results in their investigation of platelet adhesion on glass slides coated with organosilicon thin films. Hasirci[14] examined the effect of organosilicon coatings on activated charcoal (used in hemoperfusion). The coatings were deposited from hexamethyldisiloxane by PECVD. The damage to platelets, erthrocytes, and leucocytes in blood normally caused by charcoal granules was significantly reduced by the silicone coating.

Some of the characteristics of silicones are more desirable than those of fluorocarbons for biopassivation applications. Most importantly, the chemical nature of silicones enables covalent bond formation with the native silicon dioxide layer on silicon substrates, creating excellent adhesion.[15] The high strength of a covalently bonded interface is desired for long-term protection of the surface. Furthermore, silicone polymers synthesized by CVD have a lower degree of surface roughness compared to fluorocarbon films.[16] Having smooth surfaces is necessary to minimize tissue damage in the immediate vicinity of the implant.

Organosilicon coatings on silicon microribbons and neural probes were examined by Pryce Lewis et al. As in the case of fluorocarbon films, the PECVD technique was found to be an effective method for coating these micron-scale, three-dimensional objects. Figures

1.5 and 1.6 show PECVD organosilicon coatings on a silicon microribbon cable and a University of Michigan (UM) neural probe, respectively.

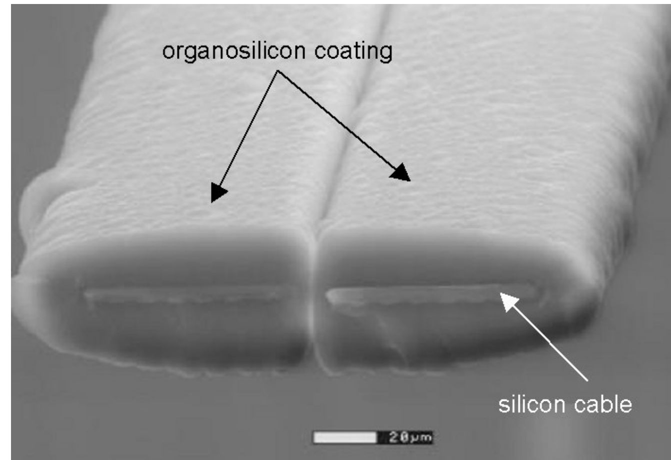

Figure 1.5 Pulsed plasma enhanced CVD organosilicon coated silicon microribbon cable.[17]

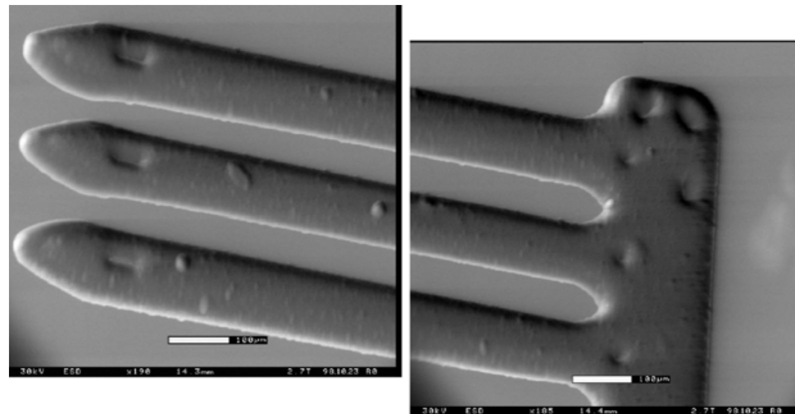

Figure 1.6 Pulsed plasma enhanced CVD organosilicon coated UM neural probe.[18]

1.5 Fluorocarbon-Organosilicon Copolymers

When considered separately, fluorocarbon and organosilicon polymers have several properties that are attractive for biopassivation applications. Fluorocarbon polymers have low dielectric constants, high resistivities, low surface energies, and high hydrophobicity. However fluorocarbon coatings have a high degree of surface roughness and their adhesion to silicon substrates is poor. Organosilicon polymers, on the other hand, adhere very well to silicon substrates and are smooth (low surface roughness). However, the electrical properties of organosilicon polymers such as dielectric constant and resistivity are not as attractive as those of fluorocarbons. A fluorocarbon-organosilicon copolymer therefore has the potential to incorporate the desirable attributes of each class of material into a single coating.

An important advantage of CVD is the ability to create copolymers that are difficult to synthesize by bulk or solution techniques, such as fluorocarbon-organosilicon copolymers. Organosilicon polymers having fluorocarbon pendant groups of the form $CH_2CH_2(CF_2)_xCF_3$ as well as polymers having short fluorocarbon segments attached to siloxane chains have been synthesized by solution chemistry techniques.[19-22] CVD offers an easier route to the production of these polymers as the process does not involve a solvent and can be performed in a single step.

Few attempts have been made to create fluorocarbon-organosilicon copolymers by CVD, and these have been limited to plasma-enhanced CVD.[23-27] Sakata et al[23] obtained thin films using hexamethyldisiloxane (HMDSO) and tetrafluoromethane (CF_4) by plasma-enhanced CVD. The structure of the films was found to be different from a simple blend of fluorocarbon and organosilicon polymers. In other words, the polymer film did not consist of

simple block or random copolymers. The authors observed the presence of Si-F bonds, and the data presented indicates that most of the fluorine in the films was bonded to silicon.

Similar results were obtained by Kim et al[24] with HMDSO and perfluorobenzene (C_6F_6). This investigation also included dielectric constant measurements and adhesion tests. The dielectric constants of the copolymer films were found to lie between those of the respective homopolymeric films, between 2 (pure fluorocarbon) and 4 (pure organosilicon). Annealing the films brought about a slight decrease in the dielectric constant. Adhesion of these films to silicon substrates was measured using the ASTM tape test[28] and was determined to be better than that of pure fluorocarbon films.

Favia et al[27] investigated the plasma-enhanced CVD of a cyclic fluorinated siloxane, (3,3,3-trifluoropropyl)methylcyclotrisiloxane. The authors examined the effects of varying substrate temperature and substrate bias on the deposition rate and chemical composition of the films. Films deposited with substrate temperatures below 200°C were determined to be structurally similar to the precursor. The carbon and hydrogen content of the films was found to decrease at higher substrate temperatures along with the deposition rate. Increasing the substrate bias resulted in greater crosslinking and higher deposition rate. The authors emphasize the absence of Si-F, Si-H and O-H bonds in their films.

In all of the above investigations, the fluorocarbon-organosilicon materials produced had poorly defined chemical structures due to the low selectivity of the PECVD technique. Having a well-defined chemical structure is essential in order to understand the structure-property-processing relationships of a material. A good understanding of these relationships is, in turn, vital for the development of a biopassivation coating that has all of the desired characteristics.

The objective of this thesis is to investigate the synthesis of fluorocarbon-organosilicon copolymer thin films using the more selective HFCVD technique and evaluate the chemical and physical properties of these films. While synthesizing an effective biopassivation coating is the primary goal of this work, this thesis also explores applications for fluorocarbon-organosilicon copolymers beyond the realm of neural prostheses.

1.6 Thesis Framework

Chapter Two reports a preliminary attempt to synthesize fluorocarbon-organosilicon copolymer thin films by HFCVD. Rigorous chemical characterization confirms the copolymeric nature of the films. The characterization methodologies described in this chapter are used extensively in subsequent chapters.

Chapter Three describes the use of an initiator in the HFCVD synthesis of fluorocarbon-organosilicon copolymers. The similarity between this HFCVD synthesis and conventional free radical polymerization in solution is highlighted.

Chapter Four examines the role of filament temperature in the HFCVD of fluorocarbon-organosilicon copolymers using an initiator. Profound differences in chemical structure are observed in the range of filament temperatures examined. These differences give rise to significant changes in thermal and mechanical properties.

Chapter Five describes a technique for grafting chains of poly(acrylamide) onto fluorocarbon-organosilicon films produced by HFCVD. This is the first step in an effort to create bioactive surface coatings by using the techniques of CVD and solution chemistry in combination.

Each technical chapter is structured as a journal article, beginning with a brief introduction, followed by a description of experimental methods, presentation of results and discussion, and finally ending with conclusions. The chapters are arranged in a manner that provides continuity within the thesis. Some additional experimental results are presented and discussed in the Appendix. The thesis concludes with a summary of the work accomplished and suggestions for future work.

1.7 References

1. Pedotti, A., Ferrarin, M., Quintern, J. and Riener, R. *Neuroprosthetics: from Basic Research to Clinical Application* (Springer-Verlag, Berlin, 1996).
2. Nichols, M. F. *Crit. Rev. Biomed. Eng.* **22**, 39 (1994).
3. Yasuda, H. *Plasma Polymerization*, (Academic Press, Orlando, Florida, 1985).
4. Wrobel, A. M. and Czeremuszkin, G. *Thin Solid Films* **216**, 203 (1992).
5. Yasuda, H. and Hsu, T. *J. Polym. Sci., Polym. Chem. Ed.* **15**, 81 (1977).
6. Limb, S. J., Edell, D. J., Gleason, E. F. and Gleason, K. K. *J. Appl. Polym. Sci.* **67**, 1489 (1998).
7. Limb, S. J., Gleason, K. K., Edell, D. J. and Gleason, E. F. *J. Vac. Sci. Technol. A* **15**, 1814 (1997).
8. Limb, S. J. Ph.D. Thesis (Massachusetts Institute of Technology, Cambridge, Massachusetts, 1997).
9. Limb, S. J., Labelle, C. B., Gleason, K. K., Edell, D. J. and Gleason, E. F. *Appl. Phys. Lett.* **68**, 2810 (1996).
10. d'Agostino, R., Cramarossa, F., Fracassi, F. and Illuzzi, F. in *Plasma Deposition, Treatment, and Etching of Polymers* (ed. d'Agostino, R.) 95 (Academic Press, San Diego, 1990).
11. Gombotz, W. R. and Hoffman, A. S. *Crit. Rev. Biocompat.* **4**, 1 (1987).

12. Chawla, A. S. *Biomaterials* **2**, 83 (1981).
13. Ishikawa, Y., Sasakawa, S., Takase, M., Iriyama, Y. and Osada, Y. *Makromol. Chem., Rapid Commun.* **6**, 495 (1985).
14. Hasirci, N. *J. Appl. Polym. Sci.* **34**, 2457 (1987).
15. Wrobel, A. M. and Wertheimer, M. R. in *Plasma Deposition, Treatment, and Etching of Polymers* (ed. d'Agostino, R.) 163 (Academic Press, San Diego, 1990).
16. Murthy, S. K. and Gleason, K. K. *unpublished results*
17. Pryce Lewis, H. G., Edell, D. J. and Gleason, K. K. *Chem. Mater.* **12**, 3488 (2000).
18. Pryce Lewis, H. G. and Gleason, K. K. *unpublished results*
19. Owen, M. J. and Kobayashi, H. *Macromol. Symp.* **82**, 115 (1994).
20. Owen, M. J. in *Block Copolymers Science and Technology* (ed. Meier, D. J.) **3**, 129 (MMI Press, Midland, 1983).
21. Doeff, M. M. and Lindner, E. *Macromolecules* **22**, 2951 (1989).
22. Chen, G. J. and Tamborski, C. *J. Organomet. Chem.* **293**, 313 (1985).
23. Sakata, J., Yamamoto, M. and Tajima, I. *J. Polym. Sci. A* **26**, 1721 (1988).
24. Kim, D. S., Lee, Y. H. and Park, N. *Appl. Phys. Lett.* **69**, 2776 (1996).
25. Kitoh, H., Muroyama, M., Sasaki, M. and Iwasawa, M. *Jpn. J. Appl. Phys.* **35 (2B)**, 1464 (1996).
26. Shirafuji, T., Miyazaki, Y., Nakagami, Y., Hayashi, Y. and Nishino, S. *Jpn. J. Appl. Phys.* **38 (7B)**, 4520 (1999).
27. Favia, P., Caporiccio, G. and d'Agostino, R. *J. Polym. Sci. A* **32**, 121 (1994).
28. ASTM Designation D 3359 - 95, American Society for Testing and Materials.

Chapter Two

Fluorocarbon-Organosilicon Copolymer Synthesis by Hot Filament Chemical Vapor Deposition

S.K. Murthy and K.K. Gleason, *Macromolecules* **35**, 1967 (2002).

Abstract

Hot-filament chemical vapor deposition has been used to deposit copolymer thin films consisting of fluorocarbon and organosilicon groups from hexafluoropropylene oxide (HFPO) and hexamethylcyclotrisiloxane (D_3). This method offers an easy route to the production of such copolymers as the process does not require a solvent and can be performed in a single step. The presence of covalent bonds between the fluorocarbon and organosilicon moieties in the thin films has been confirmed by infrared spectroscopy; X-ray Photoelectron (XPS); and solid-state ^{19}F, ^{13}C and ^{29}Si nuclear magnetic resonance (NMR) spectroscopy. The film structure consists of chains with linear and cyclic siloxane groups and CF_2 groups as repeat units. Crosslinking and termination occur mainly via the siloxane units.

Acknowledgments

We gratefully acknowledge the support of the NIH under contract NO1-NS-9-2323. In addition, this work made use of MRSEC Shared Facilities supported by the NSF under award DMR-9400334. We would also like to thank Bradley D. Olsen for preparing samples for NMR analysis. B.D. Olsen was supported by the Paul E. Gray Fund for undergraduate research at MIT.

2.1 Introduction

Fluorocarbon and organosilicon thin films produced by chemical vapor deposition have a wide variety of applications, ranging from biocompatible coatings for medical implants[1-6] to low-κ dielectrics in integrated circuits.[7-13] Fluorocarbon films have been found to be biocompatible and to have low dielectric constants. Organosilicon films with cross-linked siloxane groups offer the advantage of superior thermal stability [relative to linear poly(dimethylsiloxane)].[14] Further, they adhere well to silicon substrates by means of covalent bonds formed with the native oxide on the silicon surface.[15] A fluorocarbon-organosilicon copolymer film therefore has the potential to incorporate the desirable attributes of each class of material into a single film.

Silicone or fluorocarbon homopolymers can be coated onto surfaces by a number of techniques such as spin-on coating, casting, or chemical vapor deposition. An important advantage of chemical vapor deposition (CVD) is the ability to create copolymers that are difficult to synthesize by bulk or solution techniques, such as fluorocarbon-organosilicon copolymers. Organosilicon polymers having fluorocarbon pendant groups of the form $CH_2CH_2(CF_2)_xCF_3$ as well as polymers having short fluorocarbon segments attached to siloxane chains have been synthesized by solution chemistry techniques.[16-19] CVD offers an easier route to the production of these polymers as the process does not involve a solvent and can be performed in a single step.

Among the different CVD techniques available, hot-filament CVD (HFCVD, also known as pyrolytic or hot-wire CVD) is unique in several respects. First, HFCVD does not require the generation of a plasma, thereby avoiding defects in the growing film produced by UV irradiation and ion bombardment. In addition, films produced by HFCVD have better-

defined chemical structures because there are fewer reaction pathways than in the less selective plasma-enhanced CVD method. Further, HFCVD has been shown to produce films that have low degrees of crosslinking.[20] Co-deposition of fluorocarbon and organosilicon precursors has been performed using plasma enhanced CVD methods,[21-23] but the resulting films had complex structures without clearly defined spectroscopic features.

HFCVD has been used to deposit fluorocarbon films that are spectroscopically similar to poly(tetrafluoroethylene) (PTFE),[20] as well as organosilicon films that consist of linear and cyclic siloxane repeat units.[24] The precursors used in these investigations were hexafluoropropylene oxide (HFPO) and hexamethylcyclotrisiloxane (D_3), respectively. The primary propagating unit in the fluorocarbon films was difluorocarbene, generated by the pyrolysis of HFPO. In the case of the organosilicon films, the decomposition of D_3 was postulated to occur in two ways: by the breakdown of the rings into dimethylsilanone and by methyl abstraction from the six-membered ring structure, giving rise to the linear and cyclic repeat units, respectively.

This paper describes the deposition of fluorocarbon-organosilicon copolymer thin films by HFCVD from HFPO and D_3. The copolymer films have well-resolved bonding environments and extensive spectroscopic characterization confirms the presence of covalent bonds between CF_2 groups and siloxane-based polymeric units in the film.

2.2 Experimental Section

Depositions were performed in a custom-built vacuum chamber on to silicon wafer substrates. The pressure within the chamber was controlled by a butterfly valve connected to an MKS type 252 exhaust valve controller. Substrates were placed on a stage maintained at a low temperature (15 ± 5 °C) by the circulation of chilled water through internal coils. Precursor breakdown was achieved by means of a resistively heated 0.038-cm-diameter Nichrome wire (80% nickel, 20% chromium; Omega Engineering). The frame holding the filament wire was equipped with springs to compensate for thermal expansion of the wire upon heating. The distance between the filament wire and the substrate was 1.4 cm. The filament temperature was measured by a 2.2-μm infrared pyrometer. The spectral emissivity was estimated to be 0.85 based on direct-contact thermocouple experiments.

The flow of HFPO gas (donated by DuPont) into the chamber was controlled by an MKS model 1295C mass flow controller (MFC). The silicone precursor, D_3 (Gelest) was vaporized in a stainless steel vessel that was heated to 90 ± 5 °C. The lines leading from the vessel to the vacuum chamber were maintained at 130 ± 5 °C. The flow of vapor from the vessel into the chamber was regulated by a needle valve.

Prior to the deposition of copolymer film, the filament wire was preconditioned by being heated at a constant voltage of 86.5 V and under a flow of HFPO into the reactor at 30 sccm for 20 min at a chamber pressure of 1 Torr. Following this treatment, the power to the filament was turned down over a 5-min span, and the chamber was pumped up to atmospheric pressure to facilitate cleaning and placement of a 4-in. wafer on the stage.

Depositions were performed at a filament temperature of 620°C and a chamber pressure of 1 Torr. The precursor flow rates were 20 sccm for HFPO and 28 sccm for D_3.

The duration of these depositions ranged between 10 and 30 min. The deposition rate, determined by profilometry, was approximately 250 Å/min.

Fourier-transform infrared (FTIR) spectroscopy was performed on the deposited films using a Nicolet Magna 860 spectrometer in transmission mode. The spectra were baseline-corrected and normalized to a thickness of approximately 7000 Å. X-ray photoelectron spectroscopy (XPS) was carried out on a Kratos Axis Ultra spectrometer using a monochromatized aluminum K α source.

Solid-state NMR spectroscopy was performed on a home-built spectrometer comprising a 6.338 T Oxford superconducting magnet and a 3.2-mm Chemagnetics magic angle sample spinning (MAS) probe. For this analysis, approximately 14 mg of film was scraped off wafers from nine 30-min depositions, and packed into a zirconia rotor of 11 mm^3 internal volume. Sample spinning at the magic angle of 54.7° was performed in order to mitigate spectral broadening due to strong homonuclear dipolar and anisotropic chemical shift effects. The sample spinning speeds were 5, 25, and 10 kHz for ^{29}Si, ^{19}F and ^{13}C, respectively.

^{29}Si NMR experiments were performed with proton cross-polarization (CP) and proton decoupling to enhance the signal and resolution from the low-natural-abundance ^{29}Si nuclei. The ^{1}H-^{29}Si CP time was 5ms (as determined by contact-time experiments performed by Pryce Lewis et al.[24]), and the 90° pulse width was 1.3 μs. ^{29}Si spectra were also obtained with fluorine cross-polarization and fluorine decoupling. The purpose of this was to determine which silicon atoms were in close proximity (<10 Å) to fluorine-containing moieties. Contact time experiments indicated that a CP time of 5 ms was sufficient to

maximize signal intensity. The 90° pulse width for these measurements was 1.2 μs. ^{29}Si chemical shifts were externally referenced to tetramethylsilane.

^{19}F NMR spectra were obtained by direct polarization with a 90° pulse width of 1.2 μs. Chemical shifts were externally referenced to trichlorofluoromethane. ^{13}C spectra were obtained by direct polarization with proton decoupling as well as direct polarization with fluorine decoupling. The 90° pulse width was 1.8 μs for both types of spectra. ^{13}C chemical shifts were externally referenced to tetramethylsilane.

2.3 Results and Discussion

Fourier Transform Infrared (FTIR) Spectroscopy. Figure 2.1 shows the FTIR spectrum of a copolymer film compared with the spectra of homopolymeric fluorocarbon and silicone films obtained from HFPO and D_3, respectively. Table 2.1 gives the absorption band assignments from the literature. All of the bands associated with the pure-fluorocarbon[20] and the pure-silicone film[24] appear in the hybrid film, although slight shifts in position occur in some of the bands.

The FTIR bands in all three HFCVD films in Figure 2.1 are relatively narrow (fwhm of ~ 60 cm^{-1} or less), aiding in the resolution of specific chemical environments. For example, the symmetric (1155 cm^{-1}) and asymmetric (1223 cm^{-1}) CF_2 stretches can be clearly resolved in Figure 2.1c. In plasma-deposited films, there is typically only one broad band in the 1100-1500-cm^{-1} region[20] resulting from overlap of several types of C-F bonding environments. The narrowness of the FTIR bands thus indicates the structural simplicity of the HFCVD copolymer films.

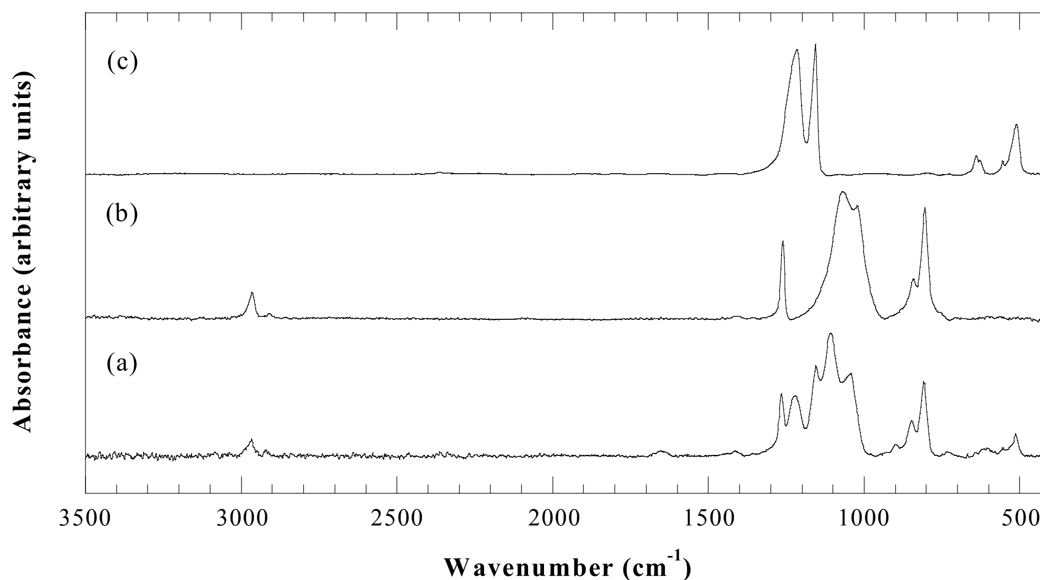

Figure 2.1 FTIR spectra of (a) copolymer, (b) silicone, and (c) fluorocarbon films, all deposited by HFCVD under the same conditions.

Table 2.1 Absorption band assignments for FTIR spectra.

assignment	copolymer (cm^{-1})	literature (cm^{-1})	ref
CF_2 rocking	514	516-520	37, 38
CF_2 wagging	610	650	39
Si-C stretching, CH_3 rocking in Si-Me_2	808	805	40
Si-C stretching, CH_3 rocking in Si-Me_3	848	845	40
Si-C stretching, CH_3 rocking in $Si(Me)_2(CF_2)$	899	N/A	N/A
Si-O-Si asymmetric stretching	1043; 1107	1050	40
CF_2 symmetric stretching	1155	1160	39
CF_2 asymmetric stretching	1223	1220	39
CH_3 symmetric bending in Si-Me_x	1265	1260	40
CH symmetric stretching in sp^3 CH_3	2913	2900	40
CH asymmetric stretching in sp^3 CH_3	2967	2960	40

The asymmetric stretching mode (ASM) of the siloxane (Si-O-Si) group is also easily resolved. The region around these bands in the copolymer spectrum is expanded for detail in Figure 2.2. The ASM appears as a doublet, as in the case of poly(dimethylsiloxane) chains with three or more siloxane units or ring structures of more than eight siloxane units.[25, 26] Both peaks of this doublet in the copolymer film (1043 and 1107 cm^{-1}) are shifted towards higher wavenumbers relative to the pure-silicone film (1020 and 1068 cm^{-1}). No shift would be expected if the fluorocarbon and organosilicon moieties were simply depositing together as two independent phases. Also, it is known[27] that electronegative substituents on the silicon atom increase the Si-O stretching frequency. Hence, the shift of the ASM is consistent with copolymerization, where bonds are formed between silicon atoms and CF_2 groups.

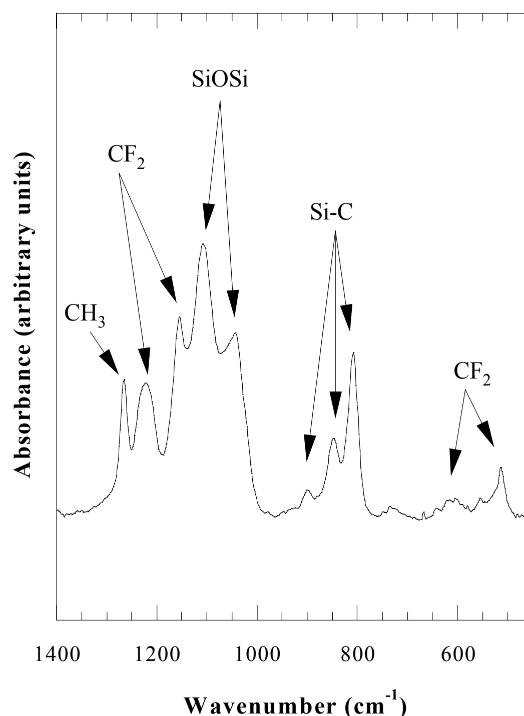

Figure 2.2 Low-wavenumber region from the FTIR spectrum of the copolymer film.

Two other modes (rocking and wagging) of the CF_2 groups appear at 514 and 610 cm^{-1} in the copolymer spectrum. The band at 610 cm^{-1} is shifted relative to its position in the pure-fluorocarbon spectrum (620 cm^{-1}). This shift towards lower wavenumbers is consistent with the shift of the ASM in the opposite direction, an effect of the redistribution of electron density caused by copolymerization.

In the pure-silicone film, Si-C stretching bands appear at 808 and 848 cm^{-1}. The copolymer spectrum contains both of these bands, as well as a third band at 899 cm^{-1}. The Si-C stretching mode is dependent on the vibrations of the substituents on the silicon atom.[28] Hence, it is likely that the band at 899 cm^{-1} is due to the Si-C stretching mode of a siloxane moiety that has both methyl and CF_2 substituents bonded to silicon.

The bands at 2913 and 2967 cm^{-1} represent the symmetric and asymmetric stretching modes of the CH bond in sp^3 CH_3 respectively. The absence of sp^3 CH_2 bands indicates that there is no crosslinking through methylene bridges.

X-Ray Photoelectron Spectroscopy. Table 2.2 summarizes atomic composition data obtained from a survey scan. The Si/O ratio is approximately 1:1.13. The high-resolution Si (2p) scan (not shown) contains a single peak with no apparent shoulders. The line width of this peak is slightly larger than that for a film deposited under the same conditions using D_3 only. Hence, while the Si/O ratio suggests that the silicon atoms in the copolymer film are almost entirely in the +2 oxidation state, the line width of the Si (2p) peak indicates the possibility of a small concentration of different oxidation states.

A C 1s high-resolution scan (Figure 2.3) indicates the presence of only two types of carbon moieties, CF_2 and CH_3. The respective assignments at 290.0 eV and 282.8 eV were made using data obtained from pure-fluorocarbon and pure-silicone films. The assumption

that most of carbon present is in the form of either CF_2 or CH_3 will greatly simplify the process of making peak assignments in the NMR spectra.

The XPS survey scan also detected small amounts of nickel and chromium in the film (<1.5 atomic %). Because no copolymer film was produced with a tantalum filament of equivalent diameter under the same conditions, this observation suggests that Nichrome plays a catalytic role in the process.

Table 2.2 XPS survey scan data.

binding energy (eV)	element	atomic concentration (%)
101	Si (2p)	13.55
283	C (1s)	30.70
531	O (1s)	15.33
576	Cr (2p)	0.48
687	F (1s)	38.42
859	Ni (2p)	1.53

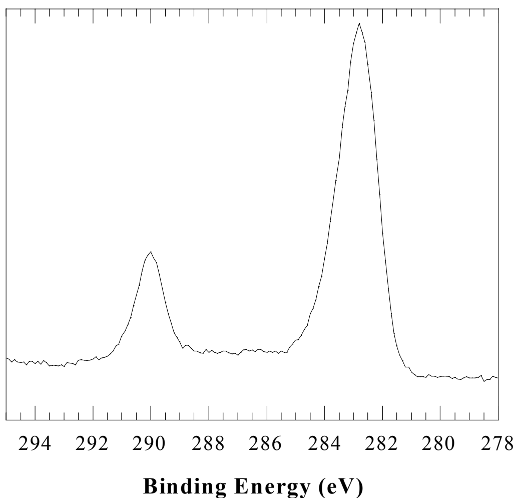

Figure 2.3 Carbon (1s) high-resolution scan of the HFCVD copolymer film showing CF_2 and CH_3 peaks.

Solid-State Nuclear Magnetic Resonance Spectroscopy. The ^{19}F NMR spectrum of the copolymer film is shown in Figure 2.4, with spinning sidebands labeled by asterisks. The remaining seven peaks represent resolved isotropic chemical shifts for fluorine. The chemical shift assignments are listed in Table 2.3. ^{19}F spectra of homopolymeric fluorocarbon films deposited by the same technique[20] show three peaks: $CF_2CF_2^*CF_2$ at –123 ppm, $CF_3CF_2^*CF_2$ at –128 ppm, and $CF_3^*CF_2$ around –84 ppm. All three of these peaks are present in Figure 2.4.

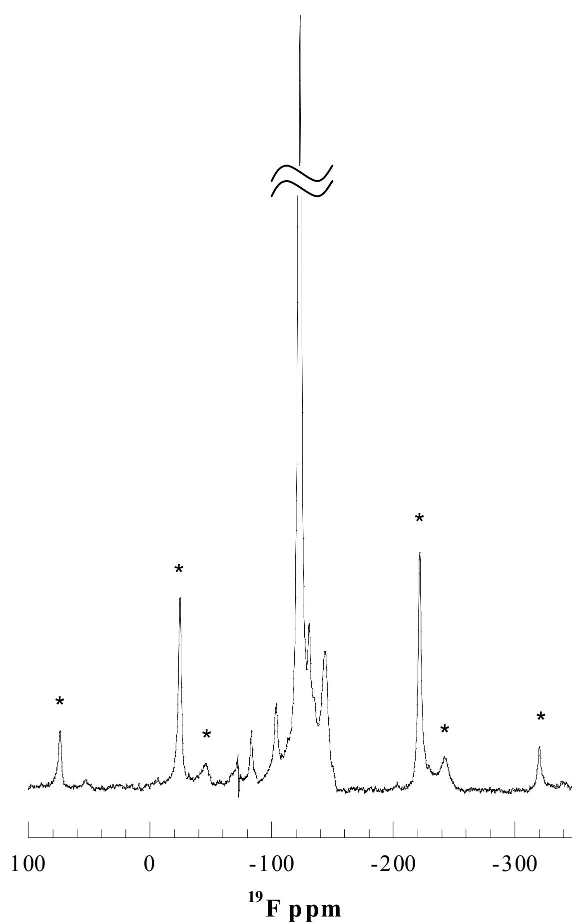

Figure 2.4 Solid-state ^{19}F NMR spectrum of the HFCVD copolymer film. The feature at -72 ppm is a spectrometer artifact.

Table 2.3 Chemical shift assignments for the ^{19}F NMR spectrum.

chemical shift (ppm)	structure	% area	ref
-83.6	$CF_3^*CF_2$	1.65	41-47
-104.5	CF_2^*O	2.97	48
-123.4	$CF_2CF_2^*CF_2$	70.30	41-47
-128.0	$CF_3CF_2^*CF_2$	0.08	41-47
-131.1	$CF_2CF_2^*Si$	6.27	29
-135.3	$CF_3CF_2^*Si$	1.10	29
-144.4	$SiCF_2^*Si$	17.63	29

The assignments for the peaks at –131.1, –135.3 and –144.4 ppm are based on chemical shifts reported for various Si-CF_2 environments in perfluoro(alkylsilanes) by Sharp et al.[29] It is postulated that these peaks correspond to $CF_2CF_2^*Si$, $CF_3CF_2^*Si$, and $SiCF_2^*Si$, respectively. The side bands that appear at –46 and –243 ppm are associated with the $SiCF_2^*Si$ peak, indicating a broad chemical shift tensor and a lack of mobility of the fluorine atoms in this environment. The ^{19}F spectrum also indicates the presence of a small number of CF_2O linkages (-104.5 ppm). These linkages could form as a result of copolymerization of CF_2 units and linear siloxane chains.

The presence of Si-CF_3 linkages was ruled out on the basis of ^{19}F and ^{19}Si NMR experiments performed on a model compound [CF_3-Si-$(CH_3)_3$]. The observed ^{19}F and ^{29}Si shifts for this compound were –27.8 and –36.2 ppm, respectively.

Figure 2.5 shows the ^{13}C NMR spectra obtained with ^{1}H and ^{19}F decoupling. Chemical shift assignments for these spectra are summarized in Table 2.4. Assignments for peaks i-iii

are taken from the literature.[30-34] In these spectra, the CH_3 and CF_2 peaks are the most intense; hence, the NMR analysis of the bulk film is in qualitative agreement with the surface analysis by C (1s) high-resolution XPS (Figure 2.3). As expected, the CH_3 peak is narrowest in the proton-decoupled spectrum, while the CF_2 and CF_3 peaks are narrowest in the fluorine-decoupled spectrum. There is a small amount of CF_3, evidenced by the presence of a shoulder on the peak at 118.6 ppm.

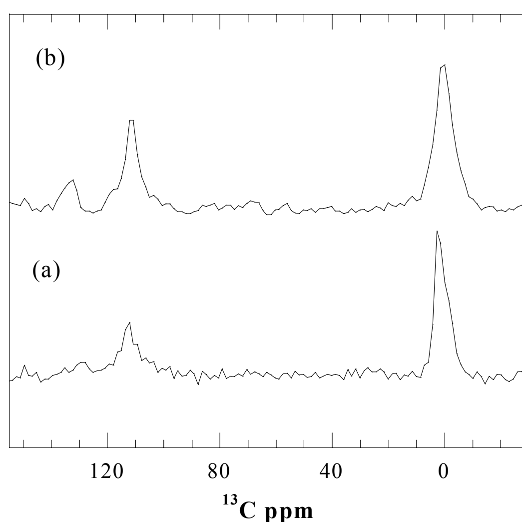

Figure 2.5 Solid-state ^{13}C NMR spectra of the HFCVD copolymer film obtained with (a) ^{1}H and (b) ^{19}F decoupling.

Table 2.4 Chemical shift assignments for the ^{13}C NMR spectra.

peak	chemical shift (ppm)	structure	% area
i	0	CH_3	62.0
ii	112	CF_2	29.4
iii	119	CF_3	1.1
iv	131	$Si – CF_2 – Si$	7.5

Given the appreciable content of $SiCF_2*Si$ in the ^{19}F spectrum, it seems likely that this moiety would also appear in the ^{13}C spectra. The peak at 131 ppm narrows considerably under fluorine decoupling and is therefore postulated to represent the $SiCF_2Si$ moiety. This hypothesis was tested by performing the calculation described below.

In the ^{19}F spectrum, the contribution of fluorine atoms to the $SiCF_2Si$ (peak area/2) was divided by the sum of the contributions from all of the fluorine atoms [(sum of all CF_2 peak areas)/2 + CF_3 peak area/3]. From the ^{13}C spectrum, the peak area of $SiCF_2Si$ was divided by the total area occupied by fluorocarbon groups (peaks ii-iv). The resulting values are in agreement (within 10%), supporting the respective assignments in the ^{19}F and ^{13}C spectra. These assignments are further substantiated by the ^{19}F and ^{13}C NMR data reported for a related molecule (FMe_2Si-CF_2-$SiMe_2F$) by Fritz and Bauer.[35] However, this type of linkage does not account for all of the CF_2 groups in the film as the ^{19}F NMR spectrum indicates that a significant fraction of the CF_2 groups is linked to other fluorocarbon groups. The possibility of having CF_2 chains that are not linked to any organosilicon moiety cannot be ruled out.

The ^{29}Si NMR spectra obtained with ^{1}H and ^{19}F cross-polarization and dipolar decoupling (CP/DD) are shown in Figure 2.6, with the peak assignments listed in Table 2.5. Although the CP/DD method increases sensitivity, the peak areas do not yield quantitative concentrations. This is in contrast to the ^{19}F and ^{13}C NMR spectra, which were obtained by direct polarization. The limited amount of film available precluded the use of direct polarization for ^{29}Si NMR spectroscopy.

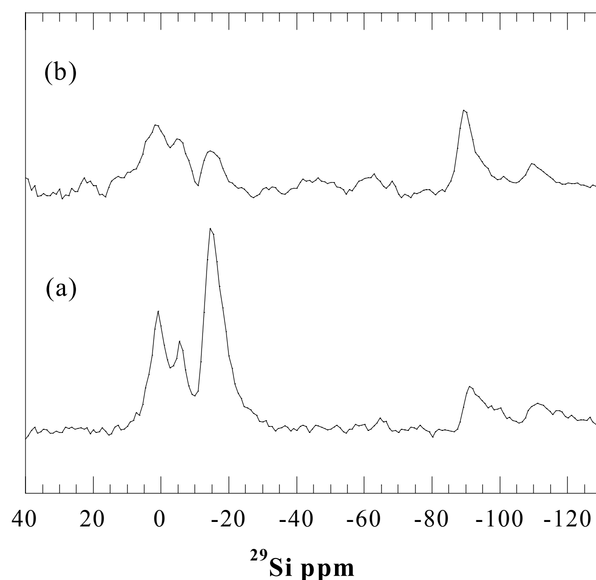

Figure 2.6 Solid-state ^{29}Si NMR spectra of the HFCVD copolymer film obtained with (a) ^{1}H and (b) ^{19}F cross-polarization and decoupling.

Table 2.5 Chemical shift assignments for the ^{29}Si NMR spectra.

chemical shift (ppm)	structure
0	$(CH_3)_2Si(O)(CF_2)$
-6.4	*o*-R_3
-15.5	$(O)_2Si(CH_3)_2$
-92.0	$(O)_2Si(CF_2)_2$
-112.0	$(O)_3Si(CF_2)$

The narrowing effect of ^{1}H decoupling is greatest for the peaks at 0, -6.4 and –15.5 ppm, indicating that these silicon environments are in the vicinity of hydrogen. The most intense of these peaks (-15.5 ppm) is assigned to the D unit [$(O)_2Si(CH_3)_2$)] assuming a small

shift relative to its –19 ppm position in spectra of films deposited from pure D_3.[24] This downfield shift is attributed to the effect of electronegative CF_2 groups bonded to neighboring siloxane groups and is consistent with the shifts observed in the FTIR spectrum of the copolymer (Figure 2.1c). Assuming a similar downfield shift, the peak at –6.4 ppm is assigned to the *o*-R_3 environment in the copolymer film.

o-R_3 represents a ring structure of three siloxane units that is bound to the film structure by Si-Si bonds. The presence of these groups is attributed to a reaction pathway involving abstraction of one or more methyl groups in D_3 with retention of the ring structure.[24] The absence of peaks at –9 and –19 ppm suggests that all of the siloxane ring structures have some degree of fluorocarbon substitution.

The peak at 0 ppm is assigned to linear siloxane units with two methyl groups and one CF_2 unit bonded to each silicon atom. The proposed bonding to CF_2 is consistent with the 0 ppm peak being the most prominent of the three peaks in this portion of the ^{19}F cross-polarized and decoupled spectrum (Figure 2.6b). Also, because the CF_2 group is less electronegative than oxygen, this moiety must lie between the M group (Me_3SiO, typically observed at +6 ppm[36]) and the D group (-15.5 ppm). The combination of one CF_2 group and one oxygen atom would, however, cause the silicon atom to appear as Si^{+2} in the XPS spectrum. The FTIR band at 899 cm^{-1} is probably due to the Si-C stretching mode in this moiety.

The peak at –92.0 ppm is most enhanced by ^{19}F cross polarization and decoupling, indicating that CF_2 and silicon are in close proximity. This peak is assigned to the $(O)_2Si(CF_2)_2$ moiety, as the large number of fluorine atoms would cause such an enhancement. The assignment is supported by the reported position of the $(SiO)_4Si^*$

(commonly known as "Q") moiety in the literature (-105 to -110 ppm).[36] Replacing two of the oxygen atoms with less-electronegative CF_2 groups would cause a downfield shift. The peak at –112.0 ppm is believed to be due to the $(O)_3Si^*(CF_2)$ moiety, which bears a closer resemblance to the Q group. The peak is sharper in the ^{19}F cross-polarized spectrum, indicating that it must be proximate to a fluorocarbon group. The oxidation state of silicon in $(O)_3Si(CF_2)$ is +3, and the intensity of the peak indicates that only a very small amount is present. This is probably why it is not easily resolved in the Si(2p) high-resolution scan.

Film Structure. The repeat units in the copolymer film consist of fluorocarbon units, siloxane units, and linkages between them. Spectroscopic data indicate that the fluorocarbon content of the films is almost entirely in the form of CF_2 and that siloxane D units are present in both linear and cyclic form. There are four distinct types of copolymer linkages. The $Si\text{-}CF_2Si$ linkage can be present between siloxane rings or between rings and linear siloxane groups. The $(CH_3)_2Si(CF_2)(O)$ link is linear, and could act as a junction between linear siloxane segments and fluorocarbon units. $(O)_2Si(CF_2)_2$ units are branch points, and can be present in siloxane rings or in linear chains. The $(O)_3Si(CF_2)$ unit, which is present in low concentrations, is a cross-linking group. The presence of these different copolymer linkages suggests that the copolymer is random.

All of the siloxane rings in the film have some degree of CF_2 substitution, and hence these can also be considered as cross-linking groups and branch points. As there is no evidence of tertiary carbon, cross-linking and branching occur entirely via these siloxane moieties.

Chain termination takes place primarily with siloxane rings (Si-Si bonding between the repeat unit and the terminating ring). Termination could also occur by means of CF_3CF_2Si or $CF_3CF_2CF_2$, but the concentration of these linkages is small.

2.4 Conclusions

Fluorocarbon-organosilicon copolymer thin films can be synthesized by hot-filament CVD from HFPO and D_3. Spectroscopic data (from XPS and FTIR and solid-state NMR spectroscopies) indicate the presence of covalent bonds between the fluorocarbon and siloxane repeat units. The data also allow for the identification of different copolymer linkages. The film structure consists of chains with linear and cyclic siloxane groups, and CF_2 groups as repeat units. Cross-linking and termination occur mainly via the siloxane units.

2.6 References

1. Noort, R. v. and Black, M. M. in *Biocompatibility of Clinical Implant Materials* (eds. Williams, D. F.) **2**, 79 (CRC Press, Boca Raton, 1981).
2. Chawla, A. S. *Artif. Organs* **3**, 92 (1979).
3. Chawla, A. S. *Biomaterials* **2**, 83 (1981).
4. Ocumpaugh, D. E. and Lee, H. L. in *Biomedical Polymers* (eds. Rembaum, A.and Shen, M.) 101 (Marcel Dekker, Inc., New York, 1971).
5. Thomson, L. A., Law, F. C., James, K. H. and Rushton, N. *Biomaterials* **12**, 781 (1991).

6. Guidoin, R., Chakfe, N., Maurel, S., How, T., Batt, M., Marois, M. and Gosselin, C. *Biomaterials* **14**, 678 (1993).
7. Moore, J. A. and Lang, C.-I. in *Fluoropolymers* (eds. Hougham, G., Cassidy, P., and Johns, K.) **1**, 273 (Kluwer Academic/Plenum Publishers, New York, 1999).
8. Hougham, G., Tesoro, G. and Viehbeck, A. *Macromolecules* **29**, 3453 (1996).
9. Lau, K. K. S. and Gleason, K. K. *Mater. Res. Soc. Symp. Proc.* **544**, 209 (1999).
10. Rosenmayer, T. and Wu, H. *Mater. Res. Soc. Symp. Proc.* **427**, 463 (1996).
11. Peters, L. *Semicond. Int.* **23**, 108 (2000).
12. Loboda, M. J. *Microelect. Eng.* **50**, 15 (2000).
13. Grill, A. and Patel, V. *J. Appl. Phys.* **85**, 3314 (1999).
14. Michalczyk, M. J., Farneth, W. E. and Vega, A. J. *Chem. Mater.* **5**, 1687 (1993).
15. Wrobel, A. M. and Wertheimer, M. R. in *Plasma Deposition, Treatment, and Etching of Polymers* (ed. d'Agostino, R.) 234 (Academic Press, San Diego, 1990).
16. Owen, M. J. and Kobayashi, H. *Macromol. Symp.* **82**, 115 (1994).
17. Owen, M. J. in *Block Copolymers Science and Technology* (ed. Meier, D. J.) **3**, 129 (MMI Press, Midland, 1983).
18. Doeff, M. M. and Lindner, E. *Macromolecules* **22**, 2951 (1989).
19. Chen, G. J. and Tamborski, C. *J. Organomet. Chem.* **293**, 313 (1985).
20. Limb, S. J., Lau, K. K. S., Edell, D. J., Gleason, E. F. and Gleason, K. K. *Plasmas and Polymers* **4**, 21 (1999).
21. Sakata, J., Yamamoto, M. and Tajima, I. *J. Polym. Sci. A* **26**, 1721 (1988).
22. Shirafuji, T., Miyazaki, Y., Nakagami, Y., Hayashi, Y. and Nishino, S. *Jpn. J. Appl. Phys.* **38** (7B), 4520 (1999).
23. Kim, D. S., Lee, Y. H. and Park, N. *Appl. Phys. Lett.* **69**, 2776 (1996).
24. Pryce Lewis, H. G., Casserly, T. B. and Gleason, K. K. *J. Electrochem. Soc.* **148** (12), F212 (2001).
25. Richards, R. E. and Thompson, H. W. *J. Chem. Soc.* **124** (1949).
26. Wright, N. and Hunter, M. J. *J. Am. Chem. Soc.* **69**, 803 (1947).

27. Lin-Vien, D., Colthup, N., Fatteley, W. G. and Grasselli, J. G. *The Handbook of Infrared and Raman Characteristic Frequencies of Organic Molecules*, (Academic Press, New York, 1991).
28. Matsurra, H., Ohno, K., Sato, T. and Murata, H. *J. Mol. Struct.* **52**, 13 (1979).
29. Sharp, K. G., Li, S. and Johannesen, R. B. *Inorg. Chem.* **15**, 2295 (1976).
30. Ovenall, D. W. and Chang, J. J. *J. Magn. Reson.* **25**, 361 (1977).
31. Kaplan, S. and Dilks, A. *J. Appl. Polym. Sci.: Appl. Polym. Symp.* **38**, 105 (1984).
32. Mallouk, T., Hawkins, B. L., Conrad, M. P., Zilm, K., Maciel, G. E. and Bartlett, N. *Philos. Trans. R. Soc. Lond. A* **314**, 179 (1985).
33. Schwerk, U., Engelke, F., Kleber, R. and Michel, D. *Thin Solid Films* **230**, 102 (1993).
34. Hagaman, E. W., Murray, D. K. and Cul, G. D. D. *Energy Fuels* **12**, 399 (1998).
35. Fritz, G. and Bauer, H. *Angew. Chem. Int. Ed. Engl.* **22**, 730 (1983).
36. Marsmann, H. in *NMR: Oxygen-17 and Silicon-29* (eds. Diehl, P., Fluck, E., and Kosfeld, R.) **17**, 65 (Springer-Verlag, New York, 1981).
37. Moynihan, R. E. *J. Am. Chem. Soc.* **81**, 1045 (1959).
38. Liang, C. Y. and Krimm, S. *J. Chem. Phys.* **25**, 563 (1956).
39. d'Agostino, R., Cramarossa, F., Fracassi, F. and Illuzzi, F. in *Plasma Deposition, Treatment, and Etching of Polymers* (ed. d'Agostino, R.) 95 (Academic Press, San Diego, 1990).
40. Rau, C. and Kulisch, W. *Thin Solid Films* **249**, 28 (1994).
41. Emsley, J. W. and Phillips, L. *Prog. NMR Spectrosc.* **7**, 1 (1971).
42. Dec, S. F., Wind, R. A. and Maciel, G. E. *Macromolecules* **20**, 2754 (1987).
43. English, A. D. and Garza, O. T. *Macromolecules* **12**, 351 (1979).
44. Harris, R. K. and Jackson, P. *Chem. Rev.* **91**, 1427 (1991).
45. Kitoh, H., Muroyama, M., Sasaki, M. and Iwasawa, M. *Jpn. J. Appl. Phys.* **35** (2B), 1464 (1996).
46. Tonelli, C. and Tortelli, V. *J. Fluorine Chem.* **67**, 125 (1994).
47. Tortelli, V., Tonelli, C. and Corvaja, C. *J. Fluorine Chem.* **60**, 165 (1993).
48. Banks, R. E. *Fluorocarbons and their Derivatives*, 2nd ed., 237 (MacDonald Technical and Scientific, London, 1970).

Chapter Three

Initiation of Cyclic Vinylmethylsiloxane Polymerization in a Hot-Filament Chemical Vapor Deposition Process

S.K. Murthy, B.D. Olsen, and K.K. Gleason, *Langmuir* **18**, 6424 (2002).

Abstract

The role of an initiator (perfluorooctane sulfonyl fluoride, PFOSF) in the polymerization of 1,3,5-trivinyl-1,3,5-trimethylcyclotrisiloxane (V_3D_3) by hot-filament chemical vapor deposition (HFCVD) has been demonstrated. Use of the initiator allows rapid deposition of films at significantly lower filament temperatures. Polymerization is initiated when radical species produced by the pyrolysis of PFOSF react with V_3D_3. Chain propagation occurs along the vinyl bonds of V_3D_3, resulting in chains with hydrocarbon backbones and siloxane rings as pendant groups. Chains are terminated by fluorocarbon radicals, sulfonyl fluoride radicals or other propagating chains.

Acknowledgments

We gratefully acknowledge the support of the National Institutes of Health under contract NO1-NS-9-2323. B.D. Olsen was supported by the Paul E. Gray Fund for undergraduate research at MIT. In addition, this work made use of MRSEC Shared Facilities supported by the National Science Foundation under Award Number DMR-9400334. We also thank Dr. Kenneth Lau for helpful discussions.

3.1 Introduction

Hot-filament chemical vapor deposition (HFCVD) is a one-step method of producing polymeric thin films by thermal decomposition of a precursor gas. Thermal decomposition is achieved using a resistively heated filament, and the radical species generated by this process undergo polymerization reactions to form a film on the cooled surface of a substrate. In comparison to plasma-enhanced CVD, HFCVD produces films with better-defined chemical structures since there are fewer reaction pathways available. HFCVD has been used to produce homopolymeric fluorocarbon[1] and organosilicon[2] films, as well as fluorocarbon-organosilicon copolymer films.[3] Fluorocarbon-organosilicon copolymers possess useful characteristics of fluorocarbon thin films (such as low surface energy and low dielectric constant) and organosilicon thin films (such as good adhesion to silicon substrates[4] and low surface roughness[2]). HFCVD is a useful synthetic technique because the process can be carried out in a single step with no solvent. The properties of the resulting copolymer thin films can be tuned by changing the chemical composition of the feed gases. In addition, HFCVD allows the deposition of conformal coatings on substrates of various types and geometries.

The use of an initiator in HFCVD allows films to be deposited at significantly higher rates and provides greater control over chemical composition and morphology. This was demonstrated by Pryce Lewis et al for fluorocarbon films deposited from hexafluoropropylene oxide (HFPO) using perfluorooctane sulfonyl fluoride (PFOSF) as an initiator.[5] In the mechanism proposed for film growth, the generation of free radicals from the pyrolysis of PFOSF is the initiation step:

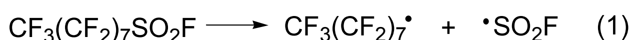
$$CF_3(CF_2)_7SO_2F \longrightarrow CF_3(CF_2)_7^{\bullet} + {}^{\bullet}SO_2F \quad (1)$$

The fluorocarbon radical subsequently combines with the propagating species, difluorocarbene (CF_2), which is generated by the pyrolysis of HFPO. The use of PFOSF resulted in higher deposition rates, more efficient utilization of HFPO, and endcapping by CF_3 groups.

This paper describes how PFOSF can be used as an initiator in the HFCVD of polymeric films from a cyclic vinylmethylsiloxane, 1,3,5-trivinyl-1,3,5-trimethylcyclotrisiloxane (V_3D_3). As in the case of fluorocarbon films, use of PFOSF allows rapid deposition of films at relatively low filament temperatures. Spectroscopic characterization shows that chain propagation occurs by polymerization across the vinyl bonds of V_3D_3. This HFCVD process thus resembles classical free radical polymerization of vinyl monomers driven by an initiator.[6] The synthetic approach described in this work can be applied to other vinyl monomers. In addition, the combination of PFOSF with V_3D_3 results in a fluorocarbon-organosilicon copolymer with unique chemical properties compared to those produced in past HFCVD work[3] or by conventional synthesis.[7-10]

3.2 Experimental Section

Film depositions were performed on silicon wafers in a custom-built vacuum chamber, as described previously.[3] For this work, the stage supporting the substrate was maintained at 25 ± 2 °C. Thermal excitation was achieved by a resistively heated 0.038-cm-diameter Nichrome wire (80% nickel, 20% chromium; Omega Engineering) without preconditioning. The filament to substrate spacing was 1.4 cm. The filament temperature was measured using a 2.2 μm infrared pyrometer with a spectral emissivity of 0.85. V_3D_3 (Gelest) was vaporized

in a stainless steel vessel that was heated to 110 ± 5 °C and fed to the reactor through a line maintained at 140 ± 5 °C. PFOSF (Aldrich) was vaporized in a glass container held at 60 ± 5 °C and fed through a line held at 90 ± 5 °C. The flow of both V_3D_3 and PFOSF into the reactor was regulated by needle valves. Depositions were carried out at a range of filament temperatures between 350 and 540 °C with a chamber pressure of 0.5 Torr. For all depositions, the flow rates of V_3D_3 and PFOSF were 23 sccm and 12 sccm respectively. Film thickness was measured by profilometry, using a Tencor P-10 Surface Profiler.

Chemical characterization was performed on a film deposited with a filament temperature of 370 °C. Fourier transform infrared (FTIR) spectroscopy was performed using a Nicolet Nexus 870 spectrometer in transmission mode. Solid-state nuclear magnetic resonance (NMR) spectroscopy was carried out using a home-built spectrometer consisting of a 6.338 T Oxford superconducting magnet and a 3.2 mm Chemagnetics magic angle sample (MAS) probe. Sample spinning speeds were 10 and 25 kHz for ^{13}C and ^{19}F, respectively. ^{13}C NMR spectra were obtained by direct polarization with proton decoupling and also by direct polarization with fluorine decoupling. The 90° pulse width was 1.8 μs for both types of spectra. ^{13}C chemical shifts were externally referenced to tetramethylsilane. ^{19}F NMR spectra were obtained by direct polarization with a 90° pulse width of 1.2 μs. ^{19}F chemical shifts were externally referenced to trichlorofluoromethane. Other experimental details have been described previously.[3]

3.3 Results and Discussion

Deposition Rate. The synthesis of organosilicon films from V_3D_3 by HFCVD using a Nichrome filament with no initiator requires filament temperatures greater than 530 °C. Under these conditions, the deposition rate is relatively low (around 100 Å/min), and deteriorates as filament age increases. Introducing PFOSF into the reaction chamber results in much higher film growth rates and allows deposition at lower filament temperatures, as indicated in Figure 3.1. Further, there is significantly less change in deposition rate over time during individual experiments.

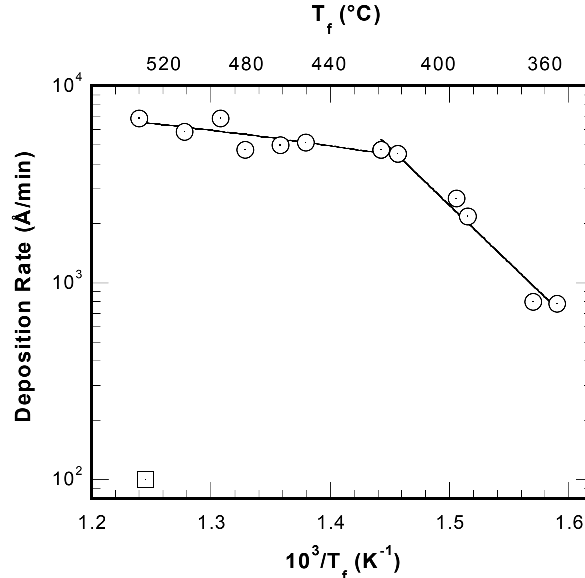

Figure 3.1 Deposition rates of HFCVD films deposited from V_3D_3 and PFOSF as a function of filament temperature (T_f). Data points marked with circles are for films deposited from V_3D_3 and PFOSF. The data point marked with a square represents a film deposited from V_3D_3 alone.

Plots such as Figure 3.1 have been used in the vapor deposition literature[5,11,12] to obtain activation energies by using Arrhenius equations to fit the data. However, such a calculation

is not justified in this instance because the deposition rate is not zero order in PFOSF in the range of filament temperatures being considered. Changing the PFOSF/V_3D_3 flow ratio does result in changes in deposition rate, indicating that the deposition rate is dependent on the concentration of PFOSF. Nevertheless, Figure 3.1 shows that there are two distinct regimes of film growth. In the region between 350 °C and 420 °C, the deposition rate is strongly influenced by filament temperature. Since films from V_3D_3 alone cannot be deposited in this filament temperature range, this suggests that film growth is initiator-limited between 350 °C and 420 °C. Above 420 °C, the increase in deposition rate is less rapid, and it is postulated that film growth is limited by mass-transfer effects. For fluorocarbon films deposited from HFPO and PFOSF, similar behavior was observed, with the transition point at 460 °C. The difference in transition temperatures is most likely due to differences in reaction kinetics.

No enhancement in deposition rate was observed when similar experiments were performed using hexamethylcyclotrisiloxane (D_3) and PFOSF as precursors. Since the only difference between the two siloxane precursors, D_3 and V_3D_3, is the presence of vinyl groups in the latter, these results indicate that vinyl groups play a critical role in initiation and subsequent film growth.

Solid-State Nuclear Magnetic Resonance Spectroscopy. Figure 3.2 shows the ^{19}F NMR spectrum of a film deposited from V_3D_3 and PFOSF at a filament temperature of 370 °C. Chemical shift assignments are given in Table 3.1. The peaks in this spectrum can be divided into three groups. The peaks between –140 and –100 ppm are due to fluorine atoms in CF_2 groups. The peaks between –100 and –50 ppm are due to fluorine atoms in CF_3 groups. The single peak at 55.6 ppm is due to fluorine atoms in SO_2F groups.

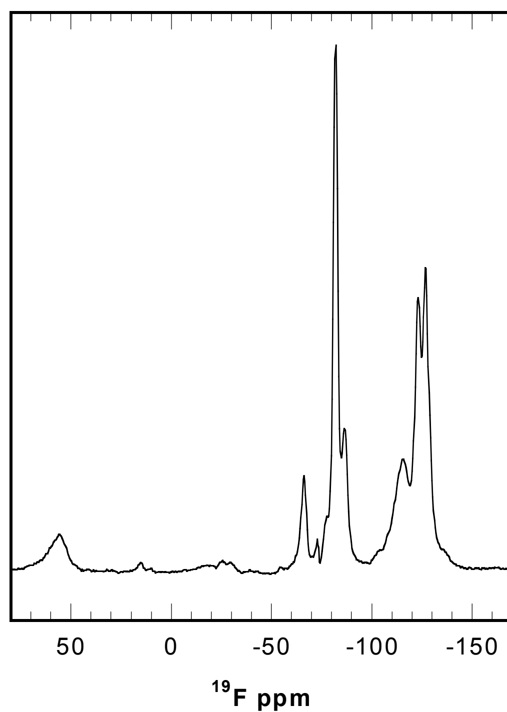

Figure 3.2 Solid-state 19F NMR spectrum of the HFCVD film deposited at a filament temperature of 370 °C. The feature at –72 ppm is a spectrometer artifact.

Table 3.1 Chemical shift assignments for the ^{19}F NMR spectrum.

peak	chemical shift (ppm)	structure	area (arbitrary units)	ref
(i)	55.6	CH(Si) SO_2F*	25.86	15
(ii)	-66.3	CF_3*-CH_2	19.50	13
(iii)	-82.1	CF_3*CF_2CF_2	100.00	16,17
(iv)	-86.3	CF_3*CF_2CH_2	21.63	13
(v)	-112.0	CF_3CF_2*CH_2	13.55	13
(vi)	-115.5	CH_2CF_2*CF_2	39.88	18
(vii)	-123.5	CF_2CF_2*CF_2	52.84	17
(viii)	-127.0	CF_3CF_2*CF_2	76.66	17

The pyrolysis of PFOSF results in the scission of the C-S bond, producing perfluorooctane radicals and sulfonyl fluoride radicals, as shown in Equation 1. The presence of $CH_2CF_2*CF_2$ (-115.5 ppm) in the ^{19}F NMR spectrum suggests that the fluorocarbon radicals formed in this pyrolysis reaction react with the vinyl groups of V_3D_3, as indicated in Equation 2. This reaction pathway offers an explanation as to why PFOSF acts an initiator on V_3D_3 but not on D_3.

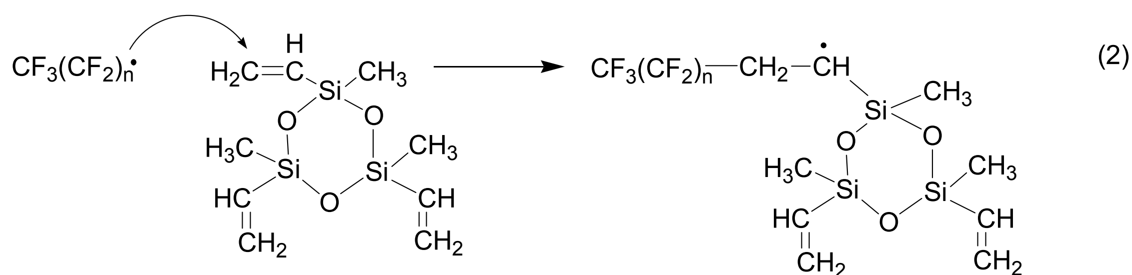

The greater width of the –115.5 ppm peak relative to the two other CF_2* peaks is attributed to the location of a second peak, the $CF_3CF_2*CH_2$ group, at –112.0 ppm.[13] The accompanying $CF_3*CF_2CH_2$ shift is observed at –86.3 ppm. The validity of these assignments was verified using the integrated peak areas listed in Table 3.1. For internal consistency, the contribution of fluorine atoms to peak iv (peak area/3) was compared with the contribution to peak v (peak area/2). An additional calculation was performed to check the consistency of peaks associated with CF_3 groups directly bonded to CF_2 groups. The fluorine contribution to peaks iii and iv (sum of peak areas/3) was compared to the contribution to peaks v and viii (sum of peak areas/2). In both calculations the values under comparison were in agreement to within 10%, supporting the respective assignments.

The appearance of the $CF_3CF_2CH_2$ group and the CF_3CH_2 group suggest that some of the perfluorooctane radicals generated by the pyrolysis of PFOSF are capable of further breakdown as shown in Reaction 3. These reactions could proceed by separation of CF_2 units from the perfluorooctane chains in the form of difluorocarbene. Alternatively, the CF_2 units could leave the chains in pairs, as tetrafluoroethylene. The radicals generated in these reactions could then react with V_3D_3 molecules by pathways analogous to Reaction 2.

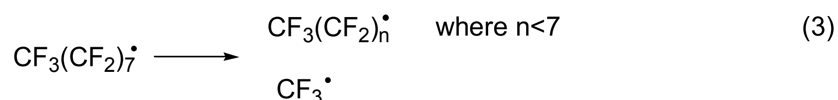

The chemical shift of fluorine atoms in SO_2F groups is between 40 and 70 ppm and depends on the nature of atoms bonded to the sulfur atom.[14] For instance, the chemical shift of $CF_2SO_2F^*$ is around 45 ppm,[15] and that of $CH_2SO_2F^*$ is approximately 53 ppm.[15] The peak at 55.6 ppm is assigned to a moiety similar to the latter, $CH(Si)SO_2F^*$. Moieties of this type would result from reactions between the free radicals generated per Reaction 2 and $\cdot SO_2F$ radicals. Since no sulfur-containing groups were observed in fluorocarbon films deposited from HFPO and PFOSF,[5] the presence of SO2F groups in these films suggests that the C-S bond is stronger when the substituents on the carbon atom are not electronegative.

Figure 3.3 shows the ^{13}C NMR of the same film obtained with ^{1}H and ^{19}F decoupling. Chemical shift assignments for these spectra are given in Table 3.2. In the absence of Reaction 3, all of the perfluorooctane radicals produced by Reaction 1 would contain 7 CF_2 groups for every CF_3 group. The ^{13}C NMR spectra indicate that the ratio of CF_2 groups to CF_3 groups is much smaller (approximately 2:1), providing support for further breakdown of these chains as given by Reaction 3. The CF_2/CF_3 ratio calculated from the ^{13}C spectra is in quantitative agreement with that calculated from the ^{19}F spectrum. The latter ratio is given

by (sum of all CF_2* peak areas/2)/(sum of all CF_3* peak areas/3). This calculation indicates that the ^{13}C spectra are consistent with the ^{19}F spectrum.

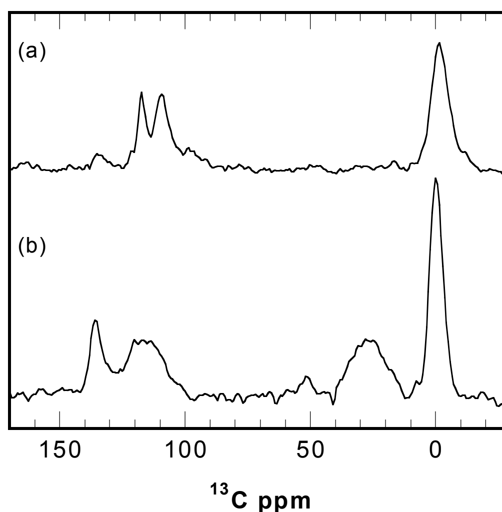

Figure 3.3 Solid-state ^{13}C NMR spectra of the HFCVD film deposited at a filament temperature of 370 °C obtained with (a) ^{19}F decoupling and (b) ^{1}H decoupling.

Table 3.2 Chemical shift assignments for the ^{13}C NMR spectra.

chemical shift (ppm)	structure	area (arbitrary units)	ref
-2 to 0	CH_3	281.30	20
12-41	CH_2 and CH(Si)	150.64	19
51.1	CH(Si)-SO_2F	12.23	15
109	CF_2	100.00	21
117	CF_3	47.88	21
135	Vinyl group	88.38	22

The broad peak between 12 and 41 ppm observed in the ^{1}H-decoupled ^{13}C spectrum is absent in the ^{19}F-decoupled spectrum, consistent with a hydrocarbon moiety with no fluorine atoms bonded to carbon. This peak lies in the region associated with CH_2 groups (5-45 ppm) as well as CH groups (25-60 ppm).[19] The presence of these groups suggests that the free radical species produced by the reaction between fluorocarbon radicals and V_3D_3 (Reaction 2) can react further with V_3D_3 molecules in a chain propagation step, as indicated in Reaction 4. Here, "I" represents any initiator fragment produced per Reaction 3.

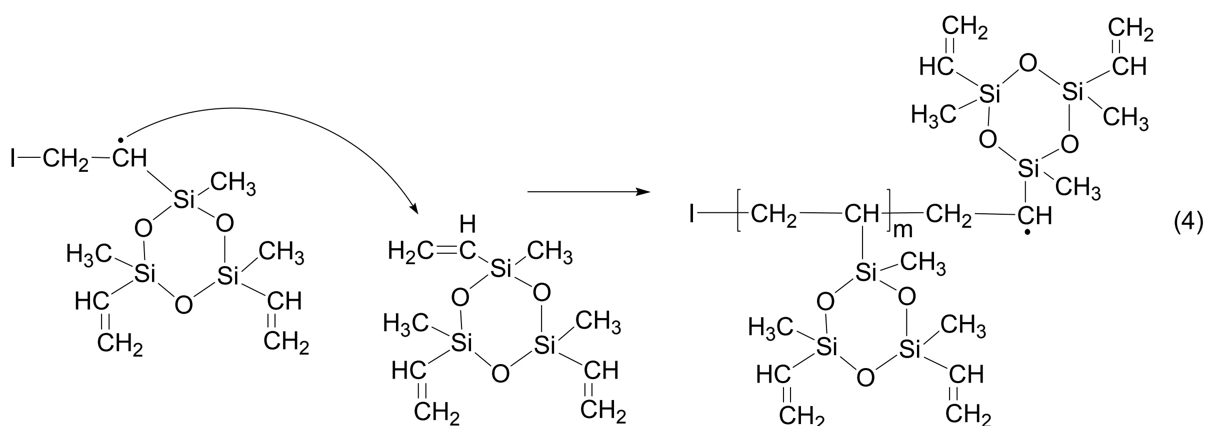

The chemical shifts of CH_2 groups and CH groups can vary significantly with position on a carbon backbone. In n-pentane, for instance, the chemical shifts of the first CH_2 group ($CH_3\underline{C}H_2CH_2CH_2CH_3$) and the second CH_2 group ($CH_3CH_2\underline{C}H_2CH_2CH_3$) are 22.8 ppm and 34.8 ppm, respectively.[19] The width of the 12-41 ppm peak is thus consistent with carbon-backbone polymer chains of varying lengths.

The peak at 51.1 ppm is assigned to the $CH(Si)SO_2F$ moiety based on the reported shift for CH_2SO_2F (47.95 ppm by Hollitzer and Sartori[15]). The presence of this peak in the ^{13}C NMR spectra is further evidence of reactions between the propagating radicals (produced per

Reactions 3 and 4) and $\cdot SO_2F$ radicals. These reactions would act as termination steps. Termination reactions could also occur by reactions between any fluorocarbon radicals and the propagating chains, or reactions between two propagating chains. The termination step is illustrated in Equation 5.

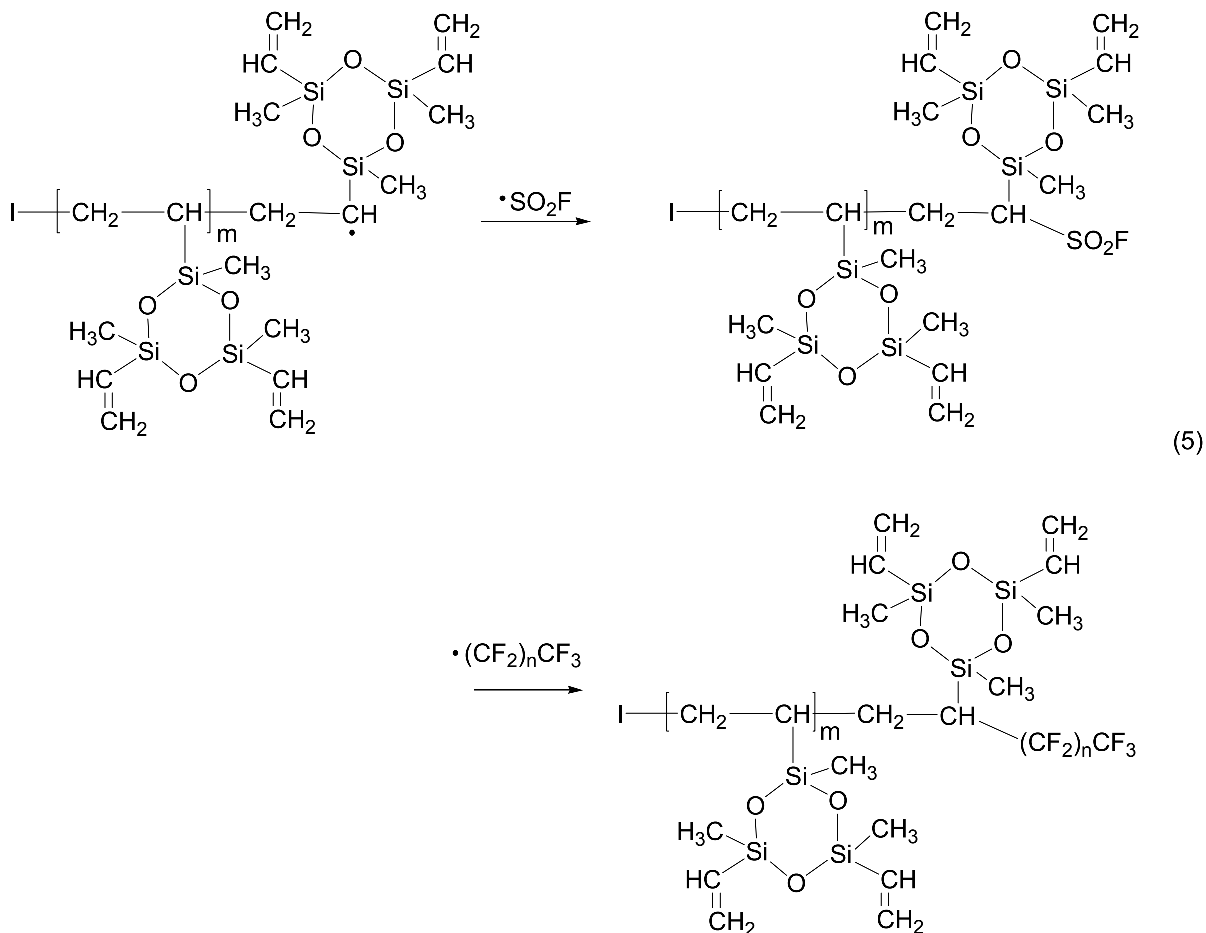

Fourier Transform Infra-Red (FTIR) Spectroscopy. Figure 3.4 shows the FTIR spectrum of the film deposited at a filament temperature of 370 °C. Absorption band assignments from the literature are given in Table 3.3. The asymmetric stretching mode (ASM) of the siloxane (Si-O-Si) group appears as a doublet with the low wavenumber band

more intense than the high wavenumber band. In their investigation of organosilicon films deposited from D_3 by HFCVD,[2] Pryce Lewis et al observed a similar trend in the ASM when the films had a greater proportion of siloxane rings relative to linear chains comprised of dimethylsiloxane groups. The trend in the ASM therefore indicates that the siloxane ring structure of V_3D_3 molecules is substantially preserved.

Bands associated with vinyl groups appear at 3060, 3020, 1599 and 614 cm^{-1}. The intensity of these bands is small in the FTIR spectrum. In fluorocarbon films deposited by HFCVD, two stretching modes of CF_2 groups are observed at around 1160 cm^{-1} and 1220 cm^{-1}.[23] These peaks appear to be shifted towards lower wavenumbers in the spectrum shown in Figure 3.4, with the former band being masked by the left-hand peak of the ASM. This shift could be caused by bonding with CH_2 groups. The conversion of vinyl groups and the shift in peak position are both consistent with Reactions 2-4.

The peak at 1409 cm^{-1} is in the region of the $=CH_2$ scissor mode, but its intensity and width suggest that it may be comprised of more than one band. This is also the region where the symmetric SO_2 stretching mode in CH_3-SO_2-F appears.[24] It is therefore postulated that the second band in this region may be due to this mode in a related moiety, the $CH(Si)SO_2F$ group.

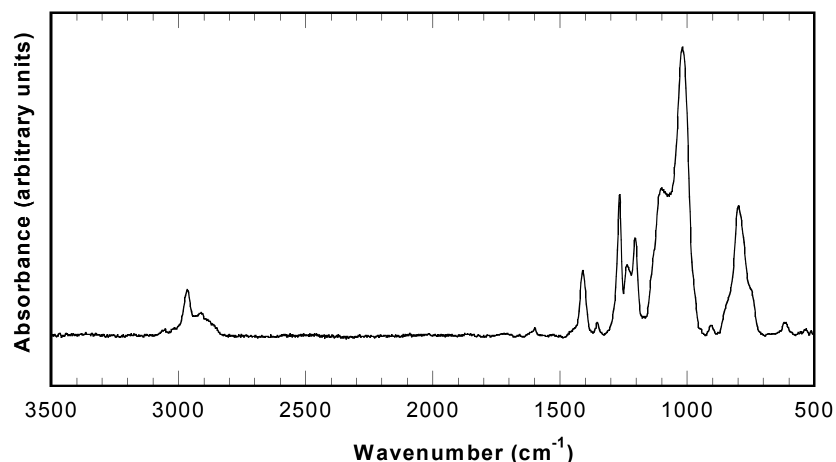

Figure 3.4 FTIR spectrum of the film deposited at a filament temperature of 370 °C.

Table 3.3 Absorption band assignments for the FTIR spectrum.

assignment	HFCVD film (cm^{-1})	literature (cm^{-1})	ref
SO_2 scissoring	575	504-586	24
$Si\text{-}CH{=}CH_2$	614	610	25
Si-C stretching, CH_3 rocking in Si(Me)(Vi)[a]	800	805	25
Si-O-Si asymmetric stretching (doublet)	1018-1104	1020-1075	2
CF_2 asymmetric stretching	1204	1220	23
CF_3-CF_2 stretching	1239	1270-1340	26
CH_3 symmetric bending in $Si\text{-}CH_3$	1265	1260	24,25
SO_2 asymmetric stretching in $CH(Si)SO_2F$,	1409	N/A	
$=CH_2$ scissoring		1400	24,25
C=C stretching in vinyl groups	1599	1600	25
C-H symmetric stretching in sp^3 CH_3	2912	2900	25
C-H asymmetric stretching in sp^3 CH_3	2967	2960	25
$=CH_2$ symmetric stretching in vinyl groups	3020	3020	25
$=CH_2$ asymmetric stretching in vinyl groups	3060	3060	25

[a] Vi denotes vinyl groups

Film Structure. The polymerization of V_3D_3 in this HFCVD process is initiated by reactions between fluorocarbon radicals and vinyl groups in the V_3D_3 molecules. Radical species generated by these reactions can react with other V_3D_3 molecules to propagate chains along vinyl bonds. These chains consist of hydrocarbon backbones with siloxane rings as pendant groups. Cross-linking between chains occurs if more than one vinyl group on any V_3D_3 molecule undergoes initiation and propagation reactions. Chain termination occurs when these propagating chains react with fluorocarbon radicals, sulfonyl fluoride radicals or with other propagating chains.

3.4 Conclusions

The role of PFOSF as an initiator in the HFCVD of films from V_3D_3 has been demonstrated. Introduction of PFOSF allows rapid deposition of films at significantly lower filament temperatures. Spectroscopic data (from FTIR and NMR spectroscopies) indicate that polymerization occurs along the vinyl bonds, leading to chains with hydrocarbon backbones and siloxane rings as pendant groups. The roles of the initiator and the vinyl groups show that this HFCVD process is analogous to classical free radical polymerization of vinyl monomers in solution.

3.5 References

1. Limb, S. J., Lau, K. K. S., Edell, D. J., Gleason, E. F. and Gleason, K. K. *Plasmas and Polymers* **4**, 21 (1999).
2. Pryce Lewis, H. G., Casserly, T. B. and Gleason, K. K. *J. Electrochem. Soc.* **148** (12), F212 (2001).
3. Murthy, S. K. and Gleason, K. K. *Macromolecules* **35**, 1967 (2002).
4. Wrobel, A. M. and Wertheimer, M. R. in *Plasma Deposition, Treatment, and Etching of Polymers* (ed. d'Agostino, R.) 163 (Academic Press, New York, 1990).
5. Pryce Lewis, H. G., Caulfield, J. A. and Gleason, K. K. *Langmuir* **17**, 7652 (2001).
6. Odian, G. *Principles of Polymerization*, (Wiley-Interscience, New York, 1991).
7. Doeff, M. M. and Lindner, E. *Macromolecules* **22**, 2951 (1989).
8. Chen, G. J. and Tamborski, C. *J. Organomet. Chem.* **293**, 313 (1985).
9. Owen, M. J. in *Block Copolymers Science and Technology* (ed. Meier, D. J.) **3**, 129 (MMI Press, Midland, 1983).
10. Owen, M. J. and Kobayashi, H. *Macromol. Symp.* **82**, 115 (1994).
11. Kubono, A. and Okui, N. *Prog. Polym. Sci.* **19**, 389 (1994).
12. Pierson, H. O. *Handbook of Chemical Vapor Deposition*, 2nd ed. (Noyes Publications, Norwich, NY, 1999).
13. Tanuma, T. and Irisawa, J. *J. Fluor. Chem.* **99**, 157 (1999).
14. Banks, R. E. *Fluorocarbons and their Derivatives*, 2nd ed. (MacDonald Technical and Scientific, London, 1970).
15. Hollitzer, E. and Sartori, P. *J. Fluor. Chem.* **35**, 329 (1987).
16. Katoh, E., Sugimoto, H., Kita, Y. and Ando, I. *J. Mol. Struct.* **355**, 21 (1995).
17. Harris, R. K. and Jackson, P. *Chem. Rev.* **91**, 1427 (1991).
18. Itoh, T., Maeda, K., Shibata, H., Tasaka, S. and Hashimoto, M. *J. Phys. Soc. Jpn.* **67**, 23 (1998).
19. Pretsch, E., Buhlmann, P. and Affolter, C. *Structure Determination of Organic Compounds*, 3rd ed. (Springer-Verlag, New York, 2000).
20. Taylor, R. B., Parbhoo, B. and Fillmore, D. M. in *The Analytical Chemistry of Silicones* (ed. Smith, A. L.) 347 (Wiley-Interscience, New York, 1991).

21. Lau, K. K. S. and Gleason, K. K. *J. Electrochem. Soc.* **146**, 2652 (1999).
22. *CRC Handbook of Chemistry and Physics* (ed. Lide, D. R.) **80**, 9-96 (CRC Press, Boca Raton, 1999).
23. d'Agostino, R., Cramarossa, F., Fracassi, F. and Illuzzi, F. in *Plasma Deposition, Treatment, and Etching of Polymers* (ed. d'Agostino, R.) 95 (Academic Press, San Diego, 1990).
24. Lin-Vien, D., Colthup, N., Fatteley, W. G. and Grasselli, J. G. *The Handbook of Infrared and Raman Characteristic Frequencies of Organic Molecules*, (Academic Press, New York, 1991).
25. Rau, C. and Kulisch, W. *Thin Solid Films* **249**, 28 (1994).
26. Labelle, C. B. and Gleason, K. K. *J. Electrochem. Soc.* **147**, 678 (2000).

Chapter Four

Effect of Filament Temperature on the Chemical Vapor Deposition of Fluorocarbon-Organosilicon Copolymers

S.K. Murthy, B.D. Olsen, and K.K. Gleason, *J. Appl. Polym. Sci.* (2003); submitted.

Abstract

The effect of filament temperature in the hot-filament chemical vapor deposition (HFCVD) of fluorocarbon-organosilicon copolymer thin films from 1,3,5-trivinyl-1,3,5-trimethylcyclotrisiloxane (V_3D_3) and perfluorooctane sulfonyl fluoride (PFOSF) has been examined. Significant changes in chemical structure occur as the filament temperature is varied, and these changes give rise to differences in thermal and mechanical properties. When the filament temperature is low, the films consist primarily of carbon-backbone polymer chains with siloxane ring pendant groups. When higher filament temperatures are used, the film structure consists of siloxane-backbone chains with some degree of crosslinking. Films produced with low filament temperatures have a greater degree of thermal stability and flexibility than those produced with high filament temperatures.

Acknowledgments

We gratefully acknowledge the support of the National Institutes of Health under contract NO1-NS2-2347. This research was also supported in part by the U.S. Army through the Institute for Soldier Nanotechnologies, under Contract DAAD-19-02-2002 with the U.S. Army Research Office. In addition, this work made use of MRSEC Shared Facilities supported by the National Science Foundation under Award Number DMR-9400334.

4.1 Introduction

Fluorocarbon and organosilicon polymers have several attributes that make them useful separately. Fluorocarbon thin films are biocompatible, hydrophobic, and have low dielectric constants.[1,2] Organosilicon thin films produced by chemical vapor deposition (CVD) have higher dielectric constants, but they are biocompatible, have low surface roughness, and adhere well to silicon substrates.[3-7] The synthesis of a fluorocarbon-organosilicon copolymer offers the opportunity to incorporate the useful characteristics of both fluorocarbon and organosilicon polymers into a single thin film. Fluorocarbon-organosilicon copolymers are currently under investigation as candidate materials for biopassivation coatings on neurological implants. These coatings need to be biocompatible, adherent, electrically insulating, and also thermally stable at the temperature of assembly of the implants (typically around 150 °C). CVD is an attractive synthetic technique for this application because it is single-step, requires no solvent, and allows coatings to be deposited on substrates with complex topographies and small overall dimensions.

In a prior investigation,[8] we described the synthesis of fluorocarbon-organosilicon copolymer thin films from hexamethylcyclotrisiloxane and hexafluoropropylene oxide by hot-filament chemical vapor deposition (HFCVD). The copolymer films had well-resolved bonding environments and the presence of covalent bonds between the fluorocarbon and siloxane polymeric units was confirmed by various spectroscopic techniques. The same synthetic method was used to demonstrate the use of an initiator, perfluorooctane sulfonyl fluoride (PFOSF), in the synthesis of fluorocarbon-organosilicon copolymer films.[9] The organosilicon precursor used in this work was 1,3,5-trivinyl-1,3,5-trimethylcyclotrisiloxane (V_3D_3). The presence of an initiator allowed deposition at relatively low filament

temperatures (370 °C), and under these conditions, chemical characterization showed that polymerization occurs across the vinyl bonds of V_3D_3. The resulting films consisted of polymer chains with carbon backbones and siloxane rings as pendant groups.

This paper examines the effect of filament temperature on the chemical and physical properties of fluorocarbon-organosilicon copolymer thin films produced from V_3D_3 and PFOSF by HFCVD. Significant changes in chemical structure are observed as the filament temperature is varied, and these changes in turn influence the mechanical and thermal properties of the films.

4.2 Experimental Section

Film depositions were carried out in a custom-built vacuum chamber described previously.[8] Precursor breakdown was achieved by use of a resistively heated 0.038-cm-diameter Nichrome wire (80% nickel, 20% chromium; Omega Engineering). The filament temperature was measured using a 2.2 μm infrared pyrometer with a spectral emissivity of 0.85. V_3D_3 (Gelest) was fed to the chamber from a stainless steel vessel heated to 110 ± 5 °C and a line maintained at 140 ± 5 °C. PFOSF (Aldrich) was vaporized in a glass container that was heated to 60 ± 5 °C and fed through a line held at 90 ± 5 °C. The flow of both precursors into the chamber was regulated by needle valves. The flow rates of V_3D_3 and PFOSF were 23 sccm and 12 sccm, respectively, and the chamber pressure was 0.5 Torr for all depositions. Substrates for the film depositions were placed on a stage within the chamber. The temperature of the stage was maintained at 25 ± 2 °C by backside water cooling.

Films were deposited on silicon wafers using filament temperatures of 370, 440, and 540 °C. For chemical characterization by solid-state nuclear magnetic resonance (NMR) spectroscopy and thermal stability studies by thermogravimetric analysis (TGA), longer duration depositions (approximately 60 minutes long) were carried out to prepare 14-16 mg samples for each of the three filament temperatures. NMR spectroscopy was performed using a home-built spectrometer consisting of a 6.338 T Oxford superconducting magnet and a 3.2 mm Chemagnetics magic angle spinning (MAS) probe. For NMR analysis, films were scraped off wafers and packed into zirconia rotors of 11 mm^3 internal volume. Sample spinning was performed at speeds of 10 kHz and 5 kHz for ^{13}C and ^{29}Si respectively. ^{13}C NMR spectra were obtained by direct polarization with proton decoupling, requiring approximately 17 hours of signal averaging per spectrum. ^{29}Si spectra were obtained with proton cross-polarization and proton decoupling, requiring approximately 25 hours of signal averaging per spectrum. Other experimental details for NMR analysis have been described previously.[8] Sample preparation for TGA was done by scraping films off wafers and loading into a platinum pan covered with aluminum foil. TGA was performed on a Perkin Elmer TGA 7 analyzer using nitrogen as the purge gas with a flow rate of 20 ml/min. Samples were held at 40 °C for 3 min and then heated to approximately 450 °C at a rate of 10 °C/min.

Films were also deposited on 50-μm-diameter platinum wires (A-M Systems). These wires were mounted on an aluminum ring with posts, and the distance between the wires and the reactor stage was 0.5 cm. The distance between the substrate wires and the Nichrome filament was 1.8 cm. The structure of the coatings was observed using a FEI/Philips XL30 environmental scanning microscope (ESEM).

4.3 Results and Discussion

^{13}C NMR Spectroscopy. Figure 4.1 shows the ^{13}C NMR spectra of the films produced at three different filament temperatures. Chemical shift assignments for these spectra are given in Table 4.1. Peak areas were obtained using a non-linear least squares regression. Since the ^{13}C NMR spectra were obtained by direct polarization, these areas provide a quantitative measure of the concentrations of the respective carbon moieties.

In our prior investigation of the chemical structure of films deposited from V_3D_3 and PFOSF at a filament temperature of 370 °C,[9] the peak between 12 and 41 ppm was shown to be evidence of carbon-backbone polymer chains with siloxane ring pendant groups. These chains are formed by chain propagation along the vinyl bonds of V_3D_3, as shown in reaction 1. Here, "I" represents a fluorocarbon initiator fragment produced by the thermal decomposition of PFOSF.[9] This initiator fragment is of the form $CF_3(CF_2)_n$ where n varies from 0-7.

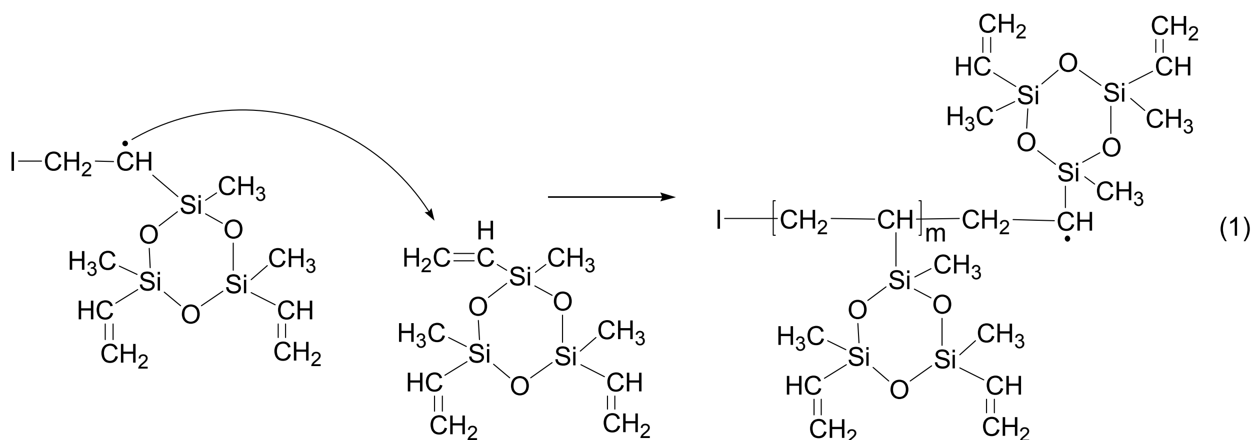

The 12-41 ppm peak corresponds to CH_2 and CH(Si) groups in the carbon backbone, and decreases in intensity as the filament temperature is increased. The peak at 135 ppm, which corresponds to unreacted vinyl groups, follows the same trend. If reaction 1 were the

only pathway available to the vinyl groups in V_3D_3, the decrease in intensity of the 135 ppm peak should be accompanied by an increase in the 12-41 ppm peak. Since both of the peaks decrease in intensity with increasing filament temperature, the ^{13}C NMR spectra suggest the presence of an alternative reaction pathway (in addition to reaction 1), which becomes more dominant at higher filament temperatures. Such a pathway could be one that involves abstraction of vinyl groups from the V_3D_3 molecules. An abstraction reaction would result in a lower intensity for the 135 ppm peak, and also leave fewer vinyl groups available for polymerization per reaction 1, thereby giving a lower intensity for the 12-41 ppm peak.

The ^{13}C NMR spectra also indicate that the methyl content of the precursor is substantially preserved in all of the films. Michalczyk et al[10] examined the thermal stability of cross-linked siloxane polymers prepared from 1,3,5,7-tetravinyl-1,3,5,7-tetramethyl-cyclotrisiloxane (V_4D_4), an eight-membered ring, and its hydrogen-substituted analog, 1,3,5,7-tetramethylcyclotetrasiloxane (H_4D_4), by thermogravimetric analysis coupled with mass spectrometry. The cleavage of Si-vinyl bonds was found to occur at a lower temperature compared to that of Si-methyl bonds. The latter was not significant at temperatures lower than 550 °C. This observation is consistent with the preferential abstraction of vinyl groups observed in the films deposited from V_3D_3 and PFOSF.

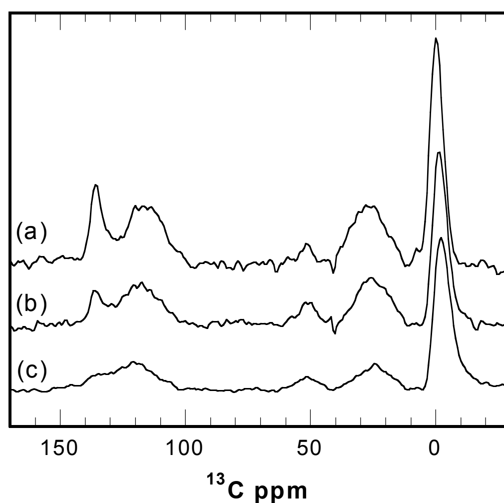

Figure 4.1 ^{13}C NMR spectra of the HFCVD films deposited at filament temperatures of (a) 370 °C, (b) 440 °C, and (c) 540°C. Spectra were obtained by direct polarization with proton decoupling.

Table 4.1 Chemical shift assignments for the ^{13}C NMR spectra of Figure 4.1.

chemical shift (ppm)	structure	normalized peak area (arbitrary units)			ref
		370 °C	440 °C	540 °C	
-2 to 0	CH_3	1.000	1.000	1.000	11
12-41	CH_2 and CH(Si)	0.536	0.468	0.220	12
51	$CH(Si)SO_2F$	0.043	0.114	0.059	13
109	CF_2	0.435	0.354	0.178	14
117	CF_3	0.208	0.219	0.161	14
135	vinyl group	0.314	0.142	0.117	15

^{29}Si NMR Spectroscopy. Figure 4.2 shows ^{29}Si NMR spectra of the same set of films, with peak assignments listed in Table 4.2. Since ^{29}Si NMR was performed using proton cross-polarization, the spectra are not quantitative and thus no peak areas are given in Table 4.2.

The ^{29}Si NMR spectrum of the precursor V_3D_3 contains only one peak at –22 ppm. This peak appears in the spectrum of the film deposited at the lowest filament temperature (Figure 4.2a), and is assigned to the vinylmethylsiloxane group in a ring structure of three siloxane units (peak iv in Table 4.2). Also present in Figure 4.2a is a peak at –10.9 ppm, which is assigned to the siloxane group in a pendant ring that is directly bonded to a carbon-backbone chain (peak i in Table 4.2; see reaction 1). Since both of the carbon atoms attached to the silicon atom of interest in this moiety are sp^3 hybridized, its chemical shift is close to the –10 ppm shift reported for the dimethylsiloxane groups in hexamethylcyclotrisiloxane.[6] As the filament temperature is increased, these two peaks are replaced by a single peak at –16.4 ppm. This peak is assigned to the linear-siloxane chain version of the $(CH_2)CH$-$Si(O)_2(CH_3)$ group.[10]

The peak lying between –31.0 and –33.7 ppm (peak v in Table 4.2) represents the vinylmethylsiloxane group in a linear chain.[16] This peak decreases in intensity with filament temperature, along with peak iv. Since both of these peaks correspond to siloxane moieties with vinyl groups, their decreasing trend indicates a greater degree of vinyl group abstraction at higher filament temperatures. This trend is consistent with the decrease in vinyl group concentration with increasing filament temperature observed in the ^{13}C NMR spectra.

The most significant effect of increasing filament temperature, however, is the increase in intensity of the peak located between –64 and –69 ppm. This peak is assigned to the

$(O)_3Si(CH_3)$ (commonly known as "T") group.[6] The formation of T groups requires abstraction of vinyl groups from the siloxane units in V_3D_3. The increasing intensity of the T group peak with increasing filament temperature is therefore indicative of greater vinyl group abstraction, and is consistent with the trends followed by peaks iv and v. The vinyl group abstraction reaction is shown in equation 2.

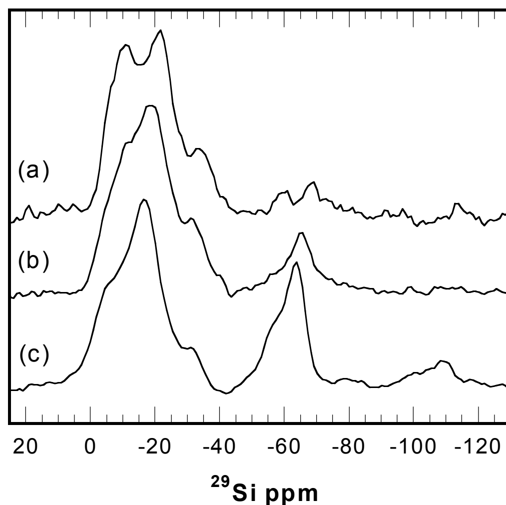

Figure 4.2 ^{29}Si NMR spectra of the HFCVD films deposited at filament temperatures of (a) 370 °C, (b) 440 °C, and (c) 540°C. Spectra were obtained with proton cross-polarization and proton decoupling.

Table 4.2 Chemical shift assignments for the ^{29}Si NMR spectra of Figure 4.2.

peak	chemical shift (ppm)	structure
i	-4.0 to –6.0	CF_2–[CH–CH_2]n–; Si*(CH_3) in ring O–Si–O–Si–O
ii	-10.9	–CH_2–[CH–CH_2]n–; Si*(CH_3) in ring O–Si–O–Si–O
iii	-16.4	–CH–CH_2–; O–Si*–CH_3; O
iv	-21.9	H_2C=CH–Si*(CH_3) in ring O–Si–O–Si–O
v	-31.0 to –33.7	H_2C=CH; O–Si*–O; CH_3
vi	-56.4 to –60.1	CF_2; O–Si–CH_3; O
vii	-63.7 to –69.2	O; O–Si*–CH_3; O
viii	-108.4 to –114.0	O; O–Si*–O; O

(2)

In addition to vinyl abstraction, a second requirement for T group formation is the creation of a third Si-O bond in the siloxane moiety produced in reaction 2. The formation of such a bond could occur by a reaction between this moiety and another V_3D_3 molecule, as shown in reaction 3. The resulting radical species is a ring structure attached to a linear vinylmethylsiloxane chain that is three monomer units in length. This moiety may react further with other V_3D_3 rings or undergo a termination reaction with a siloxane or fluorocarbon radical. Another possible reaction pathway for the formation of T groups is the decomposition of the six-membered V_3D_3 ring into three vinylmethylsilanone molecules,[17] followed by a reaction between the silanone molecules and vinyl-abstracted siloxane groups.

(3)

The reaction pathways proposed in equations 2 and 3 indicate that the formation of T groups is accompanied by the conversion of some six-membered V_3D_3 rings into linear chains. The increase in T group concentration observed at higher filament temperatures should therefore occur with a greater extent of ring opening. This is indeed what is observed in the ^{29}Si NMR spectra, in the region between –4 and –34 ppm.

FTIR Spectroscopy. Figure 4.3 shows the FTIR spectra of films for the same series of filament temperatures. Absorption band assignments made from the literature are given in Table 4.3.

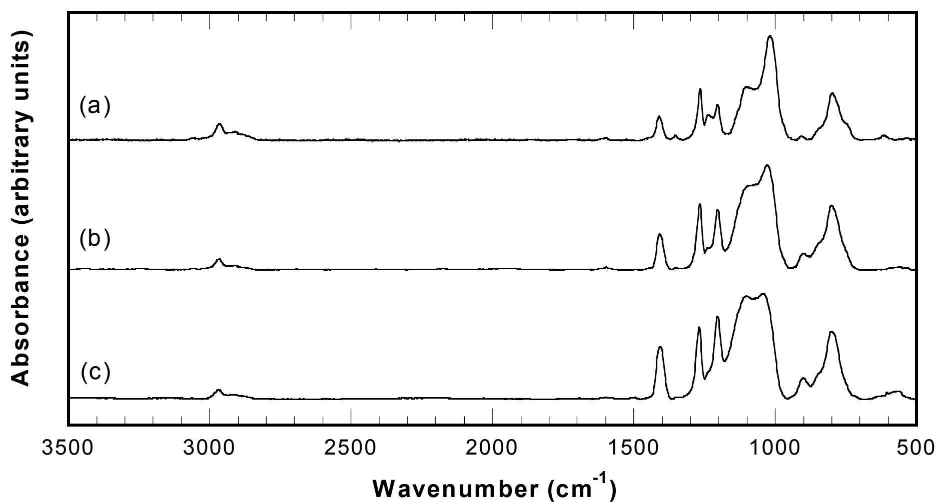

Figure 4.3 FTIR spectra of the films deposited at filament temperatures of (a) 370 °C, (b) 440 °C, and (c) 540 °C.

The asymmetric stretching mode (ASM) of the siloxane (Si-O-Si) group appears as a doublet in all of the films, indicating the presence of linear siloxane chains or ring structures.[18,19] In their investigation of organosilicon films deposited from D_3 by HFCVD,[6] Pryce Lewis et al observed a larger concentration of ring structures relative to linear chains under conditions where the lower wavenumber band of the ASM was more intense then the higher

wavenumber band. This trend in the ASM is observed in the spectrum of the copolymer film deposited at the lowest filament temperature (Figure 4.3a). As the filament temperature is increased, the relative height of the higher wavenumber band increases, indicating a transition from siloxane rings to linear siloxane chains. This is consistent with the ^{29}Si NMR data, and provides further support for the ring-opening pathway shown in equation 3.

Table 4.3 Absorption band assignments for the FTIR spectra of Figure 4.3.

assignment	HFCVD films (cm^{-1})	literature (cm^{-1})	ref
SO_2 scissoring	575	504-586	20
$Si\text{-}CH{=}CH_2$	614	610	21
Si-C stretching, CH_3 rocking in Si(Me)(Vi)[a]	800	805	21
Si-O-Si asymmetric stretching (doublet)	1018-1104	1020-1075	6
CF_2 asymmetric stretching	1204	1220	22
$CF_3\text{-}CF_2$ stretching	1239	1270-1340	23
CH_3 symmetric bending in $Si\text{-}CH_3$	1265-1270	1260-1270	20,21
SO_2 asymmetric stretching in $CH(Si)SO_2F$,	1409	N/A	
$=CH_2$ scissoring		1400	20,21
C=C stretching in vinyl groups	1599	1600	21
C-H symmetric stretching in sp^3 CH_3	2912	2900	21
C-H asymmetric stretching in sp^3 CH_3	2967	2960	21
$=CH_2$ symmetric stretching in vinyl groups	3020	3020	21
$=CH_2$ asymmetric stretching in vinyl groups	3060	3060	21

[a] Vi denotes vinyl groups

The FTIR data can also be quantitatively analyzed in conjunction with the ^{13}C NMR data to examine the relationship between vinyl group abstraction and T group formation. Figure 4.4 shows the region between 1240 cm^{-1} and 1300 cm^{-1} of the FTIR spectra for the three HFCVD films. This is the region where the symmetric bending mode of CH_3 groups in Si-CH_3 appears. The position of this band depends on the oxidation state of the silicon atom. For example, the position of this band in $O_2Si(CH_3)_2$ (commonly known as "D") groups is around 1260 cm^{-1}.[24] In T groups, where the silicon atom has a higher oxidation state, it appears around 1270 cm^{-1}.[24]

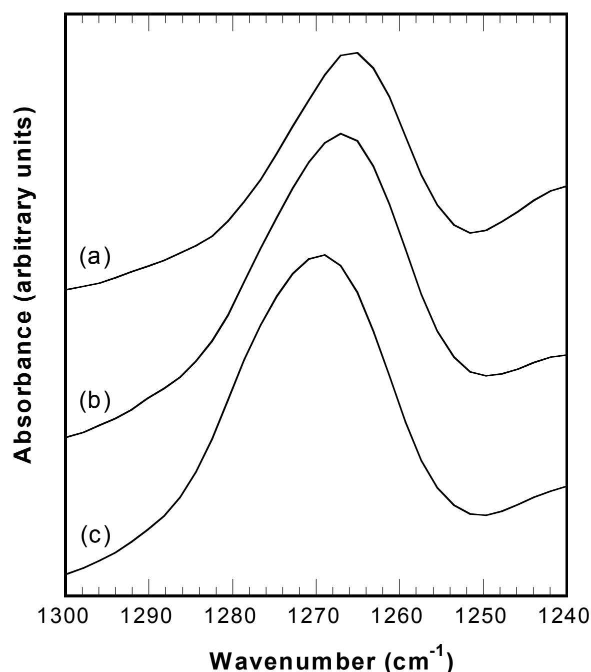

Figure 4.4 Expanded FTIR spectra of the films deposited at filament temperatures of (a) 370 °C, (b) 440 °C and (c) 540 °C showing the region of the CH_3 symmetric bending mode in Si-CH_3 groups.

In each spectrum, this band can be deconvoluted into two peaks that denote siloxane groups with silicon atoms having oxidation states of +2 and +3, respectively. The lower wavenumber peak thus represents all of the groups that are analogous to the D group (groups corresponding to peaks i-v in Table 4.2), and the higher wavenumber peak corresponds to T groups. The area under these peaks provides a measure of the concentration of the respective moieties. These areas, expressed as percentages of the overall area of the Si-CH_3 FTIR band, are given in Table 4.4 for each of the three filament temperatures.

The loss of vinyl groups from the V_3D_3 molecules can be quantified from the ^{13}C NMR data. Using the normalized areas given in Table 4.1, the lost vinyl content can be evaluated by adding the areas corresponding to the vinyl groups and the CH_2 and CH(Si) groups and subtracting the result from the area of the methyl groups. The last subtraction step is valid because the precursor V_3D_3 contains equal numbers of methyl and vinyl groups and the methyl groups do not undergo abstraction under the present conditions. The results of this calculation for all three filament temperatures are given in Table 4.4.

Table 4.4. FTIR peak fit areas and vinyl group loss quantification.

filament temperature (°C)	% D	% T	lost vinyl content (arbitrary units)
370	95.98	4.02	0.15
440	89.11	10.89	0.39
540	83.24	16.76	0.66

Comparison between the values of % T and the lost vinyl content indicate similar trends with increasing filament temperature. For example, the percentage concentration of T groups increases by a factor of 4 (approximately) as the filament temperature is increased from 370 °C to 540 °C. Over this temperature range, the degree of vinyl group loss also increases by approximately the same factor. The % T group concentration for films deposited using a filament temperature of 440 °C is about 2.7 times greater than that for films deposited using a filament temperature of 370 °C. Correspondingly, the lost vinyl content for the former is about 2.6 times greater than that of the latter. These calculations show the close relationship between vinyl group abstraction and T group formation, and support the hypothesis that the former must precede the latter, as indicated by reactions 2 and 3.

Thermal Analysis. Figure 4.5 shows the TGA results for films deposited at the three filament temperatures under consideration. The six-membered cyclic siloxane, hexamethylcyclotrisiloxane, is known to be more thermally stable than linear poly(dimethylsiloxane) (PDMS).[10] It is also known that cross-linking siloxane rings into network structures improves thermal stability.[10] In this arrangement, the siloxane rings are the repeat units, and the structure takes advantage of the superior thermal stability of the siloxane rings relative to linear PDMS. The HFCVD film deposited using a filament temperature of 370 °C is similar to this type of architecture since the structure consists primarily of carbon backbone chains with siloxane ring pendant groups. Individual siloxane rings can be connected to more than one carbon chain since more than one vinyl group on a ring can undergo polymerization. The HFCVD film deposited at 540 °C, on the other hand, is almost completely devoid of ring structures, and would therefore be expected to have lower thermal stability relative to the film deposited at 370 °C.

As anticipated, using a filament temperature of 370 °C produces a more thermally stable film than a filament temperature of 540 °C film (Figure 4.5). The film deposited with a filament temperature of 440 °C lies in-between, consistent with a mixture of rings and linear units in the film structure.

For the film deposited at a filament temperature of 370 °C, 5 % of the film mass is lost at 378 °C. For linear poly(dimethylsiloxane) (PDMS) polymers examined by Kendrick et al,[25] the estimated temperature for 5 % weight loss ranges between 340 °C and 420 °C, depending on the molecular weight of the polymer. For cross-linked siloxane glasses prepared from V_4D_4 and H_4D_4 by Michalczyk et al,[10] the temperature corresponding to 5 % weight loss was about 575 °C (these cross-linked glasses are comprised entirely of eight-membered siloxane rings linked together by methylene bridges). These values indicate that the HFCVD film deposited with a filament temperature of 370 °C is more thermally stable than low molecular weight linear PDMS chains, but not as stable as the cross-linked glasses. The preservation of siloxane ring structures is most likely the cause of the former, while the latter could be a result of insufficient ring immobilization within the film structure.

For the film deposited using a filament temperature of 540 °C, the temperature for 5 % mass loss is 324 °C. Comparison with the above mentioned value for linear PDMS suggests that this film is consists primarily of low molecular weight linear siloxane chains.

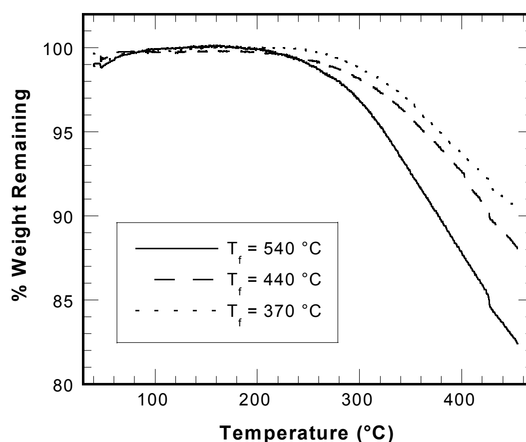

Figure 4.5 TGA results of the HFCVD films deposited at three different filament temperatures.

Wire Coatings. Figure 4.6 shows ESEM images of wire coatings made from V_3D_3 and PFOSF with filament temperatures of 370, 440, and 540 °C. The wires were tied into loops to examine the flexibility of the copolymer coating. The difference in chemical composition manifests itself in the form of brittleness, which increases as filament temperature is increased. The film deposited with a filament temperature of 540 °C cracks extensively when the wire is bent and peels off almost completely. The 440 °C coating is marginally better, and the 370 °C coating shows no apparent cracking. This trend is consistent with the brittleness observed with increasing T group concentration in organosilicon films deposited by plasma CVD by Cech et al.[26] and also with the higher rigidity of ladder-like siloxane polymers (comprised almost entirely of T groups) relative to linear polysiloxanes.[27]

This test demonstrates a qualitative similarity between these coatings and fluorocarbon coatings deposited from hexafluoropropylene oxide by Limb et al.[28] Fluorocarbon coatings

with a high degree of crosslinking were found to be more brittle than those comprised of mostly linear chains.

The increase in brittleness with filament temperature can be related to the chemical composition of the coatings using the continuous random network theory and percolation of rigidity concepts.[28-30] In a completely amorphous material consisting of random covalent bonds, the percolation of rigidity represents a threshold above which the network is said to be overconstrained and below which it is considered underconstrained.[29] This threshold is related to the average connectivity number, <r>, of the covalent network, which is defined as the average number of bonds per network forming atom. Atoms that have a valence of two or higher that are bonded to other such atoms are considered to be network forming atoms. Atoms with only one bond, such as hydrogen or fluorine, do not contribute to the network and are therefore not counted. When a material is entirely comprised of atoms that are able to form two or more bonds, the percolation of rigidity occurs at an average connectivity number of 2.4.[31] When the value of <r> is less than 2.4, the material is underconstrained, meaning that it has a low degree of cross-linking and is flexible. When <r> is greater than 2.4, the material is overconstrained and rigid.

Values of <r> for the present series of films can be estimated using the NMR and FTIR data. This is done by calculating <r> for each chemical moiety and using the composition data to determine <r> for the sample as a whole. The most significant contributions to the changes in <r> come from the siloxane moieties listed in Table 4.2.

Since the ^{29}Si NMR spectra were obtained by cross-polarization with protons, the spectra in Figure 4.2 are not quantitative. However, approximate compositions for each siloxane moiety can be obtained by using peak areas from the ^{29}Si NMR spectra along with

the quantitative FTIR data shown in Table 4.4. The first step is to assume that all of the moieties lying within the ‘D’ region of the ^{29}Si NMR spectra (-4 to –34 ppm) have the same cross-polarization efficiency. Next, fractional areas are calculated for each moiety by taking the peak area and dividing this by the sum of the areas of all peaks lying between –4 and –34 ppm. The fractional area can then be multiplied with the ‘% D’ value in Table 4.4 for the relevant filament temperature to obtain an estimate of the composition of each D-like moiety. A similar calculation can be done for each T-like moiety. The results of these calculations are shown in Tables 4.5, 4.6, and 4.7 for each of the three filament temperatures under consideration.

The next step is to calculate the value of <r> for each moiety. A general formula for <r> is given in equation 4 where n_r is the number of network forming atoms and r the number of bonds:

$$< r > = \frac{\sum_r r n_r}{\sum_r n_r} \tag{4}$$

For example, <r> = 2.57 for the moiety corresponding to peak iii in Table 4.2. In this moiety, the silicon atom has three network forming bonds (the Si-CH_3 bond is non-network forming) and each oxygen atom forms two network bonds. The –(CH-CH_2)– group is considered as a single moiety capable of forming three network forming bonds. To avoid double counting, each oxygen atoms is counted as one-half an atom, and the –(CH-CH_2)– group as one-third an atom. The numerator of equation 6 for this moiety is then $\{(3 \times 1) + (2 \times 1/2) + (2 \times 1/2) + (3 \times 1/3)\}$, and the denominator is given by the sum (1 + 1/2 + 1/2 +

1/3). Division gives <r> = 2.57. Values of <r> for each siloxane moiety are given in Tables 4.5-4.7.

Once <r> values for each moiety have been calculated, the average connectivity number for the entire sample is calculated by summing the weighted contributions from each moiety (<r> multiplied by composition value obtained from ^{29}Si NMR and FTIR) and dividing the result by the sum of the composition values. These values are also given in Tables 4.5-4.7.

The trend in the values of the average connectivity number indicates a progression from an underconstrained and flexible network to one that is overconstrained and rigid as the filament temperature is increased from 370 °C to 540 °C. This correlates well with the trend observed with the wire coatings in Figure 4.6. The coating deposited with a filament temperature of 370 °C remains intact upon bending whereas the coating deposited using a filament temperature of 540 °C undergoes extensive cracking. The electron micrographs suggest that the transition point where the percolation of rigidity occurs lies between filament temperature values of 440 °C and 370 °C. In this region, however, the values of the average connectivity number would have to lie between 2.24 and 2.16 according to the calculations. The calculated value for the transition point would then be below the threshold of 2.4 predicted by theory. This discrepancy is probably due to errors resulting from the assumption of equal cross-polarization efficiency of moieties within each group (D-like or T-like) in the ^{29}Si NMR spectra. Nevertheless, the trend in the calculated values of the average connectivity number shows the effect of increasing T group concentration on the rigidity of the wire coatings.

Table 4.5 Percolation of rigidity calculations for the HFCVD film deposited with a filament temperature of 370 °C.

^{29}Si NMR peak position (ppm)	area (arbitrary units)	fractional area	composition	<r>
-6	114188	0.148	14.17	2.57
-11	166871	0.216	20.71	2.57
-21	417858	0.540	51.85	2.00
-34	74574	0.096	9.25	2.00
-60	19384	0.310	1.25	2.40
-69	43159	0.690	2.77	2.40

Overall average connectivity number: 2.16

Table 4.6 Percolation of rigidity calculations for the HFCVD film deposited with a filament temperature of 440 °C.

^{29}Si NMR peak position (ppm)	area (arbitrary units)	fractional area	composition	<r>
-6	230332	0.164	14.59	2.57
-11	301627	0.214	19.11	2.57
-20	671576	0.477	42.54	2.00
-32	203268	0.144	12.88	2.00
-60	98437	0.401	4.37	2.40
-65	146772	0.599	6.52	2.40

Overall average connectivity number: 2.24

Table 4.7 Percolation of rigidity calculations for HFCVD film deposited with a filament temperature of 540 °C.

^{29}Si NMR peak position (ppm)	area (arbitrary units)	fractional area	composition	<r>
-6	115203	0.296	24.61	2.57
-17	255378	0.655	54.56	2.57
-32	19062	0.049	4.072	2.00
-58	78528	0.522	8.749	2.40
-64	9109	0.478	8.011	2.40
		Overall average connectivity number:		2.52

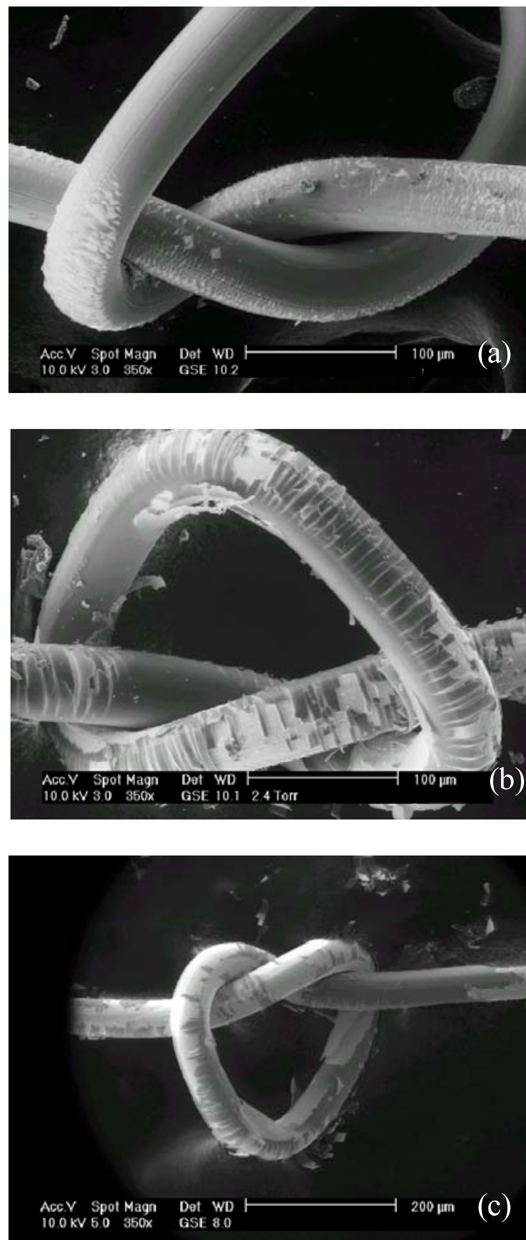

Figure 4.6 Environmental scanning electron micrographs of fluorocarbon-organosilicon copolymer wire coatings on 50 µm diameter platinum wires deposited using filament temperatures of (a) 370°C, (b) 440°C, and (c) 540°C.

4.4 Conclusions

The chemical structure of fluorocarbon-organosilicon films synthesized from V_3D_3 and PFOSF by HFCVD depends strongly on filament temperature. When the filament temperature is low, the films are comprised of carbon-backbone polymer chains with siloxane rings as pendant groups. Higher filament temperatures result in films that consist of linear siloxane chains crosslinked via T groups. This difference in chemical structure gives rise to significant differences in thermal and mechanical properties. The retention of the siloxane ring structure confers greater thermal stability on the film deposited with a low filament temperature. In addition, the chemical structure of this film is of an underconstrained nature, giving it a greater degree of flexibility. In the films deposited with higher filament temperatures, the greater concentration of T groups results in an overconstrained and brittle structure. Using a low filament temperature thus allows more selective chemistry that results in films with better properties.

4.5 References

1. Ocumpaugh, D. E. and Lee, H. L. in *Biomedical Polymers* (eds. Rembaum, A.and Shen, M.) 101 (Marcel Dekker, Inc., New York, 1971).
2. Rosenmayer, T. and Wu, H. *Mater. Res. Soc. Symp. Proc.* **427**, 463 (1996).
3. Grill, A. and Patel, V. *J. Appl. Phys.* **85**, 3314 (1999).
4. Chawla, A. S. *Artif. Organs* **3**, 92 (1979).
5. Chawla, A. S. *Biomaterials* **2**, 83 (1981).
6. Pryce Lewis, H. G., Casserly, T. B. and Gleason, K. K. *J. Electrochem. Soc.* **148** (12), F212 (2001).

7. Wrobel, A. M. and Wertheimer, M. R. in *Plasma Deposition, Treatment, and Etching of Polymers* (ed. d'Agostino, R.) 163 (Academic Press, San Diego, 1990).
8. Murthy, S. K. and Gleason, K. K. *Macromolecules* **35**, 1967 (2002).
9. Murthy, S. K., Olsen, B. D. and Gleason, K. K. *Langmuir* **18**, 6424 (2002).
10. Michalczyk, M. J., Farneth, W. E. and Vega, A. J. *Chem. Mater.* **5**, 1687 (1993).
11. Taylor, R. B., Parbhoo, B. and Fillmore, D. M. in *The Analytical Chemistry of Silicones* (ed. Smith, A. L.) 347 (Wiley-Interscience, New York, 1991).
12. Pretsch, E., Buhlmann, P. and Affolter, C. *Structure Determination of Organic Compounds*, 3rd ed. (Springer-Verlag, New York, 2000).
13. Hollitzer, E. and Sartori, P. *J. Fluor. Chem.* **35**, 329 (1987).
14. Lau, K. K. S. and Gleason, K. K. *J. Electrochem. Soc.* **146**, 2652 (1999).
15. *CRC Handbook of Chemistry and Physics* (eds. Lide, D. R.) (CRC Press, Boca Raton, 1999).
16. Zundel, T., Yu, J. M., Lestel, L., Teyssie, D. and Boileau, S. *Macromol. Symp.* **88**, 177 (1994).
17. Voronkov, M. G. *J. Organomet. Chem.* **557**, 143 (1998).
18. Richards, R. E. and Thompson, H. W. *J. Chem. Soc.* **124** (1949).
19. Wright, N. and Hunter, M. J. *J. Am. Chem. Soc.* **69**, 803 (1947).
20. Lin-Vien, D., Colthup, N., Fatteley, W. G. and Grasselli, J. G. *The Handbook of Infrared and Raman Characteristic Frequencies of Organic Molecules*, (Academic Press, San Diego, 1991).
21. Rau, C. and Kulisch, W. *Thin Solid Films* **249**, 28 (1994).
22. d'Agostino, R., Cramarossa, F., Fracassi, F. and Illuzzi, F. in *Plasma Deposition, Treatment, and Etching of Polymers* (ed. d'Agostino, R.) 95 (Academic Press, San Diego, 1990).
23. Labelle, C. B. and Gleason, K. K. *J. Electrochem. Soc.* **147**, 678 (2000).
24. Arkles, B. *Silicone Compounds Register and Review*, (Petrarch Systems, 1987).
25. Kendrick, T. C., Parbhoo, B. and White, J. W. in *The Chemistry of Organic Silicon Compounds* (eds. Patai, S.and Rappoport, Z.) **Part 2**, 1322 (John Wiley and Sons, New York, 1989).

26. Cech, V., Horvath, P., Trchova, M., Zemek, J. and Matejkova, J. *J. Appl. Polym. Sci.* **82**, 2106 (2001).
27. Timofeeva, T. V., Dubchak, I. L., Dashevsky, V. G. and Struchkov, Y. T. *Polyhedron* **3**, 1109 (1984).
28. Limb, S. J., Gleason, K. K., Edell, D. J. and Gleason, E. F. *J. Vac. Sci. Technol. A* **15**, 1814 (1997).
29. Phillips, J. C. *J. Non-Cryst. Solids* **34**, 153 (1979).
30. Thorpe, M. F. *J. Non-Cryst. Solids* **57**, 355 (1983).
31. Dohler, G. H., Dandoloff, R. and Bilz, H. *J. Non-Cryst. Solids* **42**, 87 (1980).

Chapter Five

Graft Functionalization of Fluorocarbon-Organosilicon Copolymer Thin Films

Abstract

The techniques of chemical vapor deposition (CVD) and classical solution polymerization have been used in combination to graft chains of poly(acrylamide) (PAM) onto a fluorocarbon-organosilicon copolymer thin film. This approach takes advantage of the ability of CVD to coat objects with complex topographies and small dimensions, and the versatility of solution-based techniques in the incorporation of non-volatile chemical or biological functionalities. PAM chains are covalently bonded to the fluorocarbon-organosilicon copolymer, giving rise to significant changes in surface morphology and wetting behavior. These grafted chains could potentially be modified to create bioactive surface coatings, which could be used to improve the biocompatibility and performance of biomedical implants such as neural prostheses.

Acknowledgments

We gratefully acknowledge the support of the National Institutes of Health under contract NO1-NS2-2347. This research was also supported in part by the U.S. Army through the Institute for Soldier Nanotechnologies, under Contract DAAD-19-02-2002 with the U.S. Army Research Office. In addition, this work made use of MRSEC Shared Facilities supported by the National Science Foundation under Award Number DMR-9400334. We also thank Prof. M.F. Rubner for access to the contact angle apparatus.

5.1 Introduction

Chemical vapor deposition (CVD) is a technique by which polymeric thin films can be synthesized and deposited onto a variety of substrates in a single step. An important advantage of CVD is the ability to coat substrates that have complex, three-dimensional topographies and small overall dimensions, such as micron-scale neural prostheses.[1-3] Applying conformal and reproducible coatings onto such substrates by conventional solution-based techniques is difficult because of surface tension and capillary effects. The CVD technique is, however, limited to materials whose precursors can be easily volatilized.

Biologically active coatings, such as films capable of immobilizing biomolecules like fibronectin,[4,5] laminin,[5] or DNA[6], are extremely difficult to synthesize using CVD alone because of the low volatility of the complex bioactive functional groups. Such coatings are of interest because they can enhance the biocompatibility of medical implants and improve their performance.[4,5,7] In addition, bioactive surfaces are important in the design of certain biosensors.[8,9]

CVD techniques have been used to introduce functional groups onto various types of surfaces to facilitate bonding with biological molecules. The most commonly used technique is plasma-enhanced CVD, which is also referred to as gas discharge treatment.[7,10-14] While these methods are capable of modifying the surfaces of many materials, it is desirable to have a greater degree of control over the process of introducing functional groups that are capable of bonding with biological molecules.

Bioactive coatings can be applied onto small, three-dimensional substrates by using the techniques of CVD and solution chemistry in combination. The former allows conformal coverage over complex geometries, and the latter provides the ability to work with biological

molecules. This combined approach has been used to prepare polymer surfaces for cell patterning[15] and immobilizing DNA molecules onto diamond thin films.[6] The first step in the preparation of these bioactive surfaces is the deposition of a thin film by CVD. In the next step, solution chemistry techniques are utilized to covalently attach 'conjugates' for bioactive molecules. These conjugates are molecules that can bind to biologically active species. For example, Lahann et al[15] deposited polymeric thin films from functionalized [2.2] paracyclophanes using CVD. These films were modified by attaching an amino-terminated biotin ligand, which is capable of binding with streptavidin.

In the present investigation, chains of poly(acrylamide) (PAM) have been grafted onto a fluorocarbon organosilicon copolymer film prepared by CVD. Fluorocarbon-organosilicon copolymers are being investigated as biopassivation coatings for neural prostheses because they combine the desirable properties of fluorocarbon (low dielectric constant and surface energy) and organosilicon polymers (good thermal stability and adhesion to silicon substrates). The CVD technique used to synthesize the copolymer if hot-filament CVD (HFCVD). In this technique, precursor gases are broken down by pyrolysis, and a polymeric thin film is formed on the surface of a substrate, which is maintained at room temperature.

The choice of PAM was motivated by two useful characteristics. On one hand, PAM is known to reduce protein adsorption and platelet adhesion on surfaces.[16] On the other hand, PAM can be easily hydrolyzed to poly(acrylic acid) (PAA). The carboxylic acid groups present along the backbone could then be attached to biologically active moieties such as the RGD (arginine-glycine-aspartic acid) sequence, which is known to promote cell adhesion to surfaces.[17] The latter characteristic is relevant to neural prostheses, which are designed to exchange electrical signals with neurons in the central nervous system. A surface that

promotes cell adhesion and proliferation would improve the performance of these devices while underlying fluorocarbon-organosilicon copolymer layer protects their electrical components from the ambient body environment.

5.2 Experimental Section

Fluorocarbon-organosilicon copolymer thin films were deposited onto silicon wafers by HFCVD, as described previously.[18] The precursors used were 1,3,5-trivinyl-1,3,5-trimethylcyclotrisiloxane (V_3D_3, obtained from Gelest) and perfluorooctane sulfonyl fluoride (PFOSF, obtained from Aldrich). Precursor breakdown was achieved using a Nichrome wire (80% nickel, 20% chromium; Omega Engineering) that was resistively heated to 370 °C. Organosilicon thin films were deposited from hexamethylcyclotrisiloxane (D_3) as described previously.[19]

The acrylamide monomer used in the polymerization of PAM is known to be a carcinogen and neurotoxin, and therefore appropriate precautions must be taken in handling this compound. Chemical resistant gloves, safety goggles, and appropriate skin protection (lab coat, sleeve protectors, etc.) must be worn at all times to avoid exposure. All handling of the compound should be performed only inside a chemical fume hood. The Material Safety Data Sheet (MSDS) for this compound should be consulted prior to use.

For the solution polymerization of PAM, a 16 wt./vol. % solution of acrylamide (solution 1) was first prepared in distilled water. A second solution (solution 2) containing 0.05 M sodium nitrate and 0.02 wt./vol. % sodium azide was prepared in distilled water (these compounds prevent the growth of bacteria or algae in the PAM solution). To prepare

a solution of 8 wt. % PAM, 100 mL of solution 1 and 100 mL of solution 2 were combined in a flask and mixed well. Approximately half of the mixture was then poured into a second flask. In the next step, 0.20 g of ammonium persulfate was added to one flask, and 0.10 mL of tetramethylethylene diamine was added to the other (these compounds are a redox initiator pair). Each flask was then sparged for 10 min using dry nitrogen. The contents of both flasks were then combined, mixed, and poured into a reaction vessel containing the silicon wafer coated with HFCVD film. The PAM polymerization reaction was then allowed to proceed for 30 minutes. The silicon wafer was then removed from the reaction vessel and washed thoroughly with water and acetone before drying in air. This procedure was followed with the fluorocarbon-organosilicon copolymer film as well as the homopolymeric organosilicon film.

To verify bonding between the PAM and the HFCVD copolymer film, each PAM-treated wafer was subjected to repeated washing in distilled water. Each washing cycle consisted of immersion in distilled water for 30 min followed by thorough rinsing. Up to four such cycles were performed for each sample using fresh distilled water for each cycle. An additional experiment was performed to verify that the PAM layer was covalently bonded to the underlying HFCVD film and not physically or chemically adsorbed. An aqueous solution of PAM was prepared as described above. This solution was left undisturbed overnight to ensure that the polymerization reaction was complete. Silicon wafers coated with the fluorocarbon-organosilicon copolymer by HFCVD were then immersed in the solution over a period of two days.

X-ray photoelectron spectroscopy (XPS) was performed on the un-grafted and grafted silicon wafers using a Kratos Axis Ultra spectrometer using a monochromatized aluminum K

α source. Atomic force microscopy (AFM) was carried out on a Digital Instruments Dimension 3000 microscope. Images were collected in tapping mode using a standard etched silicon tip.

The surface density of amide groups was measured by the ninhydrin method.[20] To maximize the surface area available for grafting, the HFCVD film was deposited on 0.5 mm-diameter glass beads (Biospec Products). PAM was grafted onto the coated beads by following the procedure described above. After washing and drying the beads, the PAM coating on the beads was hydrolyzed using 1.5 N hydrochloric acid at 100 °C over a span of 40 min. This reaction converts the primary amine groups to carboxylic acid groups with the release of ammonia. After cooling, excess acid was neutralized using 3.8 N sodium hydroxide to a pH of 5.5. The mixture was then filtered, and the 2.5 mL of the filtrate (taken from a total volume of 5.57 mL) was combined with 5 mL of pH 5.5 buffer (acetic acid and sodium acetate) and 2.5 mL of ninhydrin solution (0.1 M ninhydrin in ethylene glycol monomethyl ether). The ninhydrin reaction was allowed to proceed at 100 °C for 10 min. The ammonia liberated by the hydrolysis of PAM is contained in the filtrate and produces a color change upon reaction with ninhydrin. Following the ninhydrin reaction, the mixture was cooled and the absorbance at 570 nm was measured using a Milton Roy Spectronic 21 UV/VIS spectrophotometer. The concentration of NH_3 released was calculated using a calibration curve, which was obtained by performing the ninhydrin reaction with ammonia solutions of known concentration.

Contact angle measurements were made using an Advanced Surface Technologies VCA 2000 video contact angle system. A 4 μL drop of deionized water was placed on the surface and angle measurements were obtained from a video image of the drop.

5.3 Results and Discussion

HFCVD Film Structure. The chemical structure of fluorocarbon-organosilicon copolymer thin films deposited from V_3D_3 and PFOSF was examined in a prior investigation.[18] Film growth is initiated when the carbon-sulfur bond in PFOSF molecules is cleaved, resulting in fluorocarbon radicals of various lengths. These radicals can react with the vinyl groups in V_3D_3, leading to a propagation reaction as shown in Equation 1. Here, "I" represents an initiator fragment of the form $CF_3(CF_2)_n$ where n varies from 0-7. Termination of the polymer chains can occur by reaction with fluorocarbon radicals or with sulfonyl fluoride radicals.

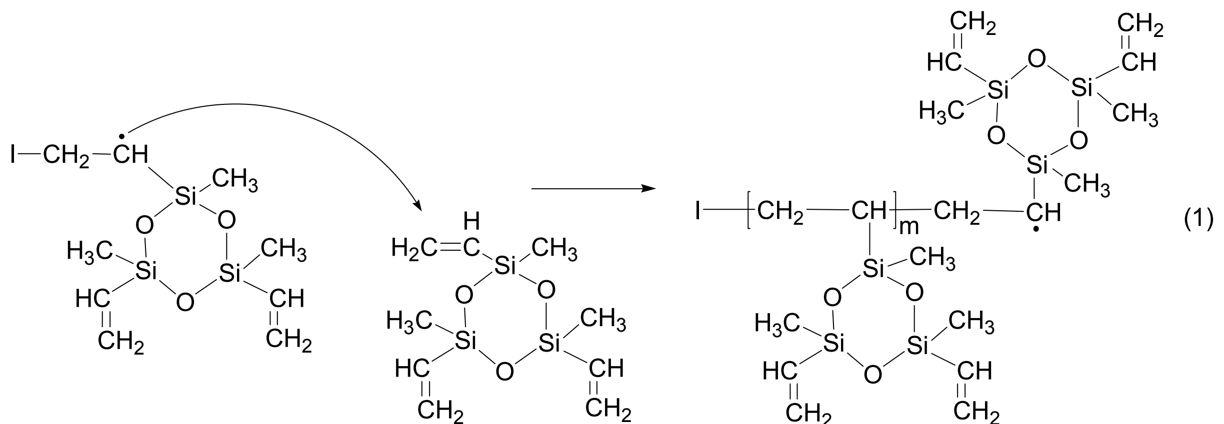

The film structure is thus comprised of polymer chains with fluorocarbon ends, hydrocarbon backbones, and siloxane rings as pendant groups. Chemical characterization by solid-state NMR indicated that there was an appreciable concentration of unreacted vinyl groups in the film.[18] The presence of these groups is essential for the grafting of PAM onto the fluorocarbon-organosilicon films.

PAM Grafting. Table 5.1 summarizes atomic composition data from XPS survey scans performed on a fluorocarbon-organosilicon copolymer film (deposited by HFCVD on a

silicon wafer) before and after PAM grafting. Higher concentrations of carbon and nitrogen after grafting suggest the presence of PAM on the film surface. Further evidence is provided by the carbon (1s) high-resolution scans shown in Figure 5.1. The carbonyl group peak is absent prior to grafting and appears after grafting. In addition, the reduction in height of the CF_2 and CF_3 peaks is consistent with the HFCVD film surface being covered by a thin layer of a different material.

Table 5.1 XPS survey scan data.

binding energy (eV)	element	atomic concentration (%)	
		before grafting	after grafting
687	F (1s)	25.95	15.43
531	O (1s)	24.94	22.66
401	N (1s)	1.69	6.88
283	C (1s)	38.19	48.18
101	Si (2p)	9.23	6.85

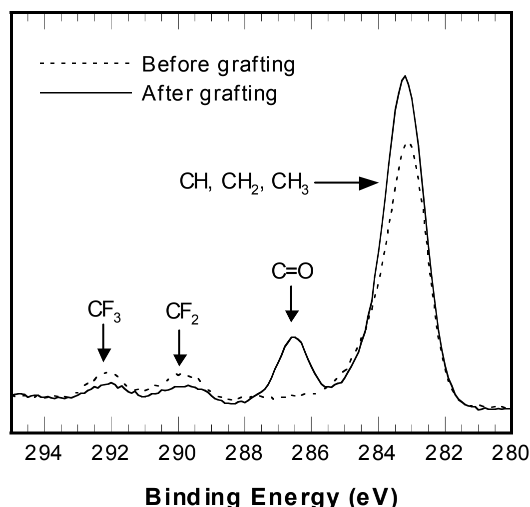

Figure 5.1 Carbon (1s) high resolution scan of the fluorocarbon-organosilicon copolymer film before and after PAM grafting. Peak assignments are taken from refs. 21 and 22. The presence of PAM on the surface is evidenced by the presence of the carbonyl group peak.

The nitrogen and carbonyl content of the PAM-grafted films was unaffected by repeated washing in distilled water. Silicon wafers coated with the fluorocarbon-organosilicon copolymer and PAM were subjected to a series of wash cycles, ranging from one to four 30-min cycles. XPS survey and carbon (1s) scans were performed after each cycle, and no reduction was observed in the concentration of nitrogen atoms and carbonyl groups. XPS analysis was also performed on fluorocarbon-organosilicon films that were immersed in aqueous solutions of PAM. In this case, the survey and carbon (1s) scans indicated that there was no adsorption of PAM onto the HFCVD film surface. These results suggest that the PAM layer is indeed covalently bonded to the fluorocarbon-organosilicon copolymer.

In the free radical polymerization of acrylamide, chain propagation occurs along the vinyl bonds of the monomer. It is therefore postulated that bonding between growing PAM chains and the HFCVD fluorocarbon-organosilicon copolymer occurs when the radical chain ends of the former react with the vinyl groups present in the latter. The critical role of vinyl groups in the grafting of PAM was confirmed by carrying out the same experiment with organosilicon films deposited by HFCVD from D_3. This precursor is similar to V_3D_3 but has no vinyl groups. The composition of the film (as determined by XPS) was the same before and after the grafting procedure.

Surface Density of Amide Groups. The ninhydrin method showed that the concentration of ammonia produced by the hydrolysis of the grafted PAM was approximately 55 ppm. For a solution volume of 5.57 mL, this means that 1.82×10^{-5} moles of amide groups were grafted onto the fluorocarbon-organosilicon copolymer film on the glass beads. Dividing this quantity by the total surface area of the beads (287.9 cm^2) gives the surface density of amide groups, which is 6.31×10^{-8} moles/cm^2 of copolymer film. Since the number of moles of amide groups must be equal to the number of moles of acrylamide units, the mass of acrylamide grafted per unit area can be calculated by multiplying the surface density by the molar mass of acrylamide. This gives a value of 4.48×10^{-6} g/cm^2. Assuming a density of 1 g/cm^3, the thickness of the PAM layer is estimated to be around 4.48×10^{-6} cm, or 44.8 nm. This calculation assumes that the PAM forms a uniform coating over the copolymer film, and should be considered as a limit. If the PAM chains are indeed attached to the copolymer film only by means of the vinyl groups present in the latter, the PAM layer would not be uniform. This would be a result of the non-uniform distribution of vinyl groups on the surface of the copolymer film.

Atomic Force Microscopy. The effect of PAM grafting on the surface morphology of the fluorocarbon-organosilicon copolymer films is shown in Figure 5.2.

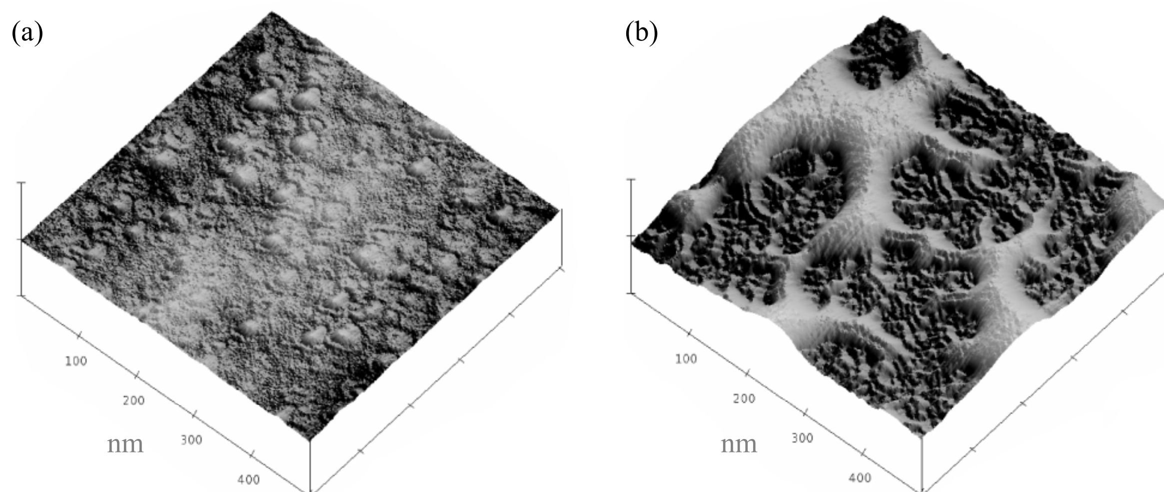

Figure 5.2 Atomic force micrographs of a fluorocarbon-organosilicon film deposited on a silicon wafer (a) before and (b) after PAM grafting. The image area for both micrographs is 500 nm^2, and the vertical scale is 35 nm/division.

The micrographs in Figure 5.2 show that the copolymer film surface is altered substantially by PAM grafting. The mountain-range-like features on the PAM-grafted films have a maximum height of approximately 30 nm. This height is close to the PAM layer thickness estimated using the ninhydrin method, suggesting that these features are comprised of PAM chains. The regions lying adjacent to these features are also different from the surface of the ungrafted film. These regions could be regions of low PAM concentration (or low molecular weight chains), while the mountain-range-like features could be regions of higher PAM concentration (or higher molecular weight chains).

Sessile Drop Contact Angles. Contact angle measurements performed on the fluorocarbon-organosilicon copolymer film before and after PAM grafting are shown in Table 5.2. In general, grafting PAM onto the HFCVD film results in lower contact angles. This is to be expected since PAM is considerably more hydrophilic than the fluorocarbon-organosilicon copolymer. The most significant effect of PAM grafting, however, is the increase in the difference between the advancing and receding contact angles. In air, the PAM chains grafted onto the HFCVD film surface are expected to be in a tightly coiled conformation. When a water drop is placed on the surface, these PAM chains would be induced to uncoil and extend themselves in order to maximize interactions between chain units and water molecules. Such a change in conformation would lower the receding contact angle. Another factor that influences contact angle hysteresis is surface roughness.[23] The AFM images in Figure 5.2 indicate that PAM grafting significantly increases the roughness of the copolymer film. This increase in roughness would contribute to the greater degree of hysteresis observed after grafting. The greater degree of uncertainty in the contact angle measurements performed on the copolymer film with PAM grafting is most likely due to the irregular distribution of PAM on the surface (Figure 5.2).

Table 5.2 Water contact angles on fluorocarbon-organosilicon copolymer film before and after PAM grafting.

sample	static (deg)	advancing (deg)	receding (deg)
copolymer film before PAM grafting	94 ± 0.8	84 ± 0.7	72 ± 0.9
copolymer film after PAM grafting	72 ± 3.7	63 ± 4.2	24 ± 4.6

5.4 Conclusions

Chains of PAM can be covalently grafted onto fluorocarbon-organosilicon copolymers synthesized by HFCVD. PAM grafting results in significant changes in surface morphology and wetting behavior. This work demonstrates the feasibility of using polymer synthesis by CVD in combination with classical solution polymerization in order to exploit the advantages of each technique. The ability to graft PAM also represents the first step in the design of a bioactive surface coating. The grafted chains of PAM could potentially be bonded to bioactive moieties to create surfaces that encourage the proliferation and growth of cells.

5.5 References

1. Murthy, S. K., Edell, D. J. and Gleason, K. K. in *Neuroprosthetics: Theory and Practice* (eds. Horch, K. W.and Dhillon, G.) (World Scientific, Singapore, 2003; in press).
2. Limb, S. J., Gleason, K. K., Edell, D. J. and Gleason, E. F. *J. Vac. Sci. Technol. A* **15**, 1814 (1997).
3. Pryce Lewis, H. G., Edell, D. J. and Gleason, K. K. *Chem. Mater.* **12**, 3488 (2000).
4. Cui, X. Y., Lee, V. A., Raphael, Y., Wiler, J. A., Hetke, J. F., Anderson, D. J. and Martin, D. C. *J. Biomed. Mater. Res.* **56**, 261 (2001).
5. Ignatius, M. J., Sawhney, N., Gupta, A., Thibadeau, B. M., Monteiro, O. R. and Brown, I. G. *J. Biomed. Mater. Res.* **40**, 264 (1998).
6. Yang, W., Auciello, O., Butler, J. E., Cai, W., Carlisle, J. A., Gerbi, J. E., Gruen, D. M., Knickerbocker, T., Lasseter, T. L., Russell, J. N., Smith, L. M. and Hamers, R. J. *Nature Mater.* **1**, 253 (2002).
7. Uyama, Y., Kato, K. and Ikada, Y. *Adv. Polym. Sci.* **137**, 1 (1998).
8. Crooks, R. M. and Ricco, A. J. *Accounts Chem. Res.* **31**, 219 (1998).
9. Mrksich, M. and Whitesides, G. M. *Trends Biotechnol.* **13**, 228 (1995).
10. Zhao, B. and Brittain, W. J. *Prog. Polym. Sci.* **25**, 677 (2000).
11. Foerch, R., McIntyre, N. S., Sodhi, R. N. S. and Hunter, D. H. *J. Appl. Polym. Sci.* **40**, 1903 (1990).
12. Hoffman, A. S. *J. Appl. Polym. Sci., Appl. Polym. Symp.* **46**, 341 (1990).
13. Hayat, U., Tinsley, A. M., Calder, M. R. and Clarke, D. J. *Biomaterials* **13**, 801 (1992).
14. Terlingen, J. G. A., Brenneisen, L. M., Super, H. T. J., Pijpers, A. P., Hoffman, A. S. and Feijen, J. *J. Biomater. Sci.-Polym. Ed.* **4**, 165 (1993).
15. Lahann, J., Balcells, M., Rodon, T., Lee, J., Choi, I. S., Jensen, K. F. and Langer, R. *Langmuir* **18**, 3632 (2002).
16. Fujimoto, K., Tadokoro, H., Ueda, Y. and Ikada, Y. *Biomaterials* **14**, 442 (1993).
17. Reed, J., Hull, W. E., Vonderlieth, C. W., Kubler, D., Suhai, S. and Kinzel, V. *Eur. J. Biochem.* **178**, 141 (1988).
18. Murthy, S. K., Olsen, B. D. and Gleason, K. K. *Langmuir* **18**, 6424 (2002).

19. Murthy, S. K. and Gleason, K. K. *Macromolecules* **35**, 1967 (2002).
20. Sano, S., Kato, K. and Ikada, Y. *Biomaterials* **14**, 817 (1993).
21. Limb, S. J., Lau, K. K. S., Edell, D. J., Gleason, E. F. and Gleason, K. K. *Plasmas and Polymers* **4**, 21 (1999).
22. Beamson, G. and Briggs, D. *High Resolution XPS of Organic Polymers*, 188-189 (John Wiley and Sons, New York, 1992).
23. Adamson, A. W. *Physical Chemistry of Surfaces*, 4th ed. (Wiley Interscience, New York, 1982).

Chapter Six

Summary and Suggestions for Future Work

6.1 Summary

This thesis has demonstrated that fluorocarbon-organosilicon copolymer thin films can indeed be synthesized by chemical vapor deposition (CVD). This work has overcome the combined challenges of copolymerizing two material types with very different chemical and physical characteristics and developing a synthetic method capable of conformally coating neural prostheses. Although more work needs to be done in order to make these copolymers viable biopassivation coatings, this research represents a significant step in that direction.

The research presented herein describes the effect of precursor choice and key experimental parameters on the chemical structure and the thermal and mechanical properties of fluorocarbon-organosilicon copolymers. The use of an initiator was shown to be an effective way to produce thin films at high growth rates with no metal incorporation. With low filament temperatures and the presence of an initiator, the mechanism of growth of the copolymer films is analogous to classical free radical polymerization in solution.

Filament temperature was observed to have a profound effect on the chemical structure of the copolymer films. Films produced with low filament temperature generally had a low degree of crosslinking whereas higher filament temperatures resulted in films with greater crosslinking. Changes in chemical structure were accompanied by changes in thermal and mechanical properties. The highly crosslinked films produced using elevated filament temperatures were less thermally stable and considerably more rigid than the films produced using low filament temperatures.

The copolymer films produced from 1,3,5-trivinyl-1,3,5-trimethylcyclotrisiloxane (V_3D_3) and perfluorooctane sulfonyl fluoride (PFOSF) using a low filament temperature appear to be the best candidates for biopassivation coatings. These films are flexible and

thermally stable beyond the desired threshold of 150 °C. They also adhere well to silicon substrates. In these respects, the copolymer films combine the desirable attributes of fluorocarbon and organosilicon homopolymers. Furthermore, the hot-filament CVD technique used to synthesize these films is compatible with the vacuum-based steps involved in the fabrication of neural prostheses.

Although wire coatings made from V_3D_3 are PFOSF are flexible, they are not completely crack-resistant. In addition, small (sub-micron scale) particles are present on the coating surface. These particles undergo corrosion when the coatings are immersed in water, suggesting that they contain trace amounts of metal incorporated from the filament wire. The formation of these particles is most likely due to flow patterns (regions of recirculation) within the CVD chamber that promote gas phase polymerization. These shortcomings can adversely affect the effectiveness of the copolymer coatings, but they are challenges that can be readily addressed in future work.

Another important accomplishment of this thesis has been to demonstrate the feasibility of using the techniques of chemical vapor deposition and solution chemistry in combination. The methodology used to graft chains of poly(acrylamide) onto fluorocarbon-organosilicon films could potentially be utilized to create bioactive surface coatings for implantable medical devices. Such coatings can be designed to promote the adhesion and proliferation of specific cell types on the device surfaces. Doing so would mitigate the effects of tissue damage caused during implantation and improve the biocompatibility and overall performance of the devices.

The research described in this thesis was driven by the need for an effective biopassivation coating on neural prostheses. The approach taken to solve this problem has

involved identifying the characteristics of an effective coating and finding ways to build those attributes into a material. This strategy has brought together fundamental concepts from vapor deposition, polymer science, and surface chemistry. The major findings of this work, such as the effect of filament temperature, use of an initiator, and the ability to graft polymers onto CVD films, illustrate how crossing disciplinary boundaries can provide rich insights into the science and technology of materials.

6.2 Suggestions for Future Work

This thesis provides insights into the synthetic chemistry and structure-property-processing relationships of fluorocarbon-organosilicon copolymer thin films. Future work must build on this knowledge and focus on properties that are particularly important from the standpoint of effective biopassivation coatings. The challenges encountered with regard to crack-resistance and particulate matter on the film surface must be addressed by making appropriate changes to the experimental conditions and CVD reactor geometry. Specifically, using lower filament temperatures and different filament materials may help to decrease the degree of cross-linking in the films deposited from V_3D_3 and PFOSF, making them more flexible. The formation of particles during the film growth process can be prevented by changing the geometry of the CVD chamber such that there are no regions of recirculation. In addition, using lower filament temperatures and a different filament material may reduce metal incorporation into the films, making them resistant to corrosion.

The chemical structure of the copolymer films and the degree of metal incorporation may also be controlled by using precursors with slightly different structures and different

pyrolysis pathways. For instance, using a cyclic siloxane precursor with fewer vinyl groups compared to V_3D_3 may help reduce cross-linking. Using a fluorocarbon initiator with a lower pyrolysis temperature than PFOSF would likely allow deposition of copolymer films at lower filament temperatures.

Once the above challenges have been overcome, the focus must shift to measuring the electrical resistance of the films upon immersion in saline solutions over extended periods of time. In addition to flat silicon substrates, coatings on various neurological electrode assembly components (such as neural probes and silicon microribbons) should also be examined.

The ability to combine solution polymerization with chemical vapor deposition presents several avenues for future research. An effective technique must be developed to determine the molecular weight of the grafted polymer chains. The possibility of attaching biological molecules (such as amino acids) to the grafted chains needs to be investigated. Such an effort may require the ability to graft other functionalities (such as carboxyl groups) to the films produced by CVD. One candidate amino acid sequence is the RGD (arginine-glycine-aspartic acid sequence) sequence, which is known to encourage cell adhesion and proliferation.[1] Successful grafting of bioactive moieties onto CVD films could lead to studies of cell adhesion and proliferation on surfaces. This work could potentially lead to the design of coatings for neural prostheses that not only protect the devices from the ambient body environment but also provide a bioactive surface to enhance device performance.

6.3 References

1. Reed, J., Hull, W. E., Vonderlieth, C. W., Kubler, D., Suhai, S. and Kinzel, V. *Eur. J. Biochem.* **178**, 141 (1988).

Appendix

Adhesion and Electrical Properties of Fluorocarbon-Organosilicon Copolymer Films

A.1 Introduction

Fluorocarbon-organosilicon copolymer thin films are being considered as candidate materials for biopassivation coatings on neural prostheses. For this application, these films must be chemically inert electrically insulating, and thermally stable at the temperature of assembly of the prosthetic devices (~ 150 °C). Furthermore, the films must adhere well to the silicon substrates that form the backbone of these devices.

In previous chapters, the chemical structure of fluorocarbon-organosilicon copolymer films produced by hot-filament chemical vapor deposition (HFCVD) has been examined in detail. Changes in chemical structure strongly influence the thermal stability and flexibility of the films.[1] Flexible and thermally stable films were obtained by depositing films from 1,3,5-trivinyl-1,3,5-trimethylcyclotrisiloxane (V_3D_3) and perfluorooctane sulfonyl fluoride (PFOSF) using low filament temperatures.[1]

This Appendix details further experiments that were performed on copolymer films deposited from V_3D_3 and PFOSF to examine adhesion to silicon substrates and electrical properties. The siloxane content of these films confers the ability to adhere well to silicon substrates. The electrical insulating ability of these films, however, is adversely affected by particles present on the film surface.

A.2 Experimental Section

Fluorocarbon-organosilicon copolymer films were deposited from V_3D_3 and PFOSF as described previously.[2] For all depositions, the chamber pressure was 0.5 Torr and the filament temperature was 370 °C. Precursor breakdown was achieved using a 0.038-cm-

diameter Nichrome wire (80% nickel, 20% chromium; Omega Engineering). V_3D_3 (Gelest) was fed to the chamber from a stainless steel vessel heated to 110 ± 5 °C and a line maintained at 140 ± 5 °C. PFOSF (Aldrich) was vaporized in a glass container that was heated to 60 ± 5 °C and fed through a line held at 90 ± 5 °C. The flow of both precursors into the chamber was regulated by needle valves.

For adhesion testing, copolymer films of two different compositions were deposited onto silicon wafers. The thickness of these films was approximately 2 μm. For the first set (referred to as the "organosilicon-rich" set), the flow rates of V_3D_3 and PFOSF into the CVD chamber were 27 sccm and 12 sccm, respectively. For the second set (referred to as the "fluorocarbon-rich" set), the flow rates of V_3D_3 and PFOSF were 23 sccm and 12 sccm, respectively. For comparison, samples of homopolymeric fluorocarbon and organosilicon films were deposited from hexafluoropropylene oxide and hexamethylcyclotrisiloxane respectively as described previously.[3] The thickness of these films was also approximately 2 μm.

Adhesion tests were performed using a Quad Group Sebastian I test unit. Alumina studs coated with epoxy were fastened onto the wafers using clamps (studs and clamps provided by Quad Group). These assemblies were then placed inside a vacuum oven maintained at 125 °C for two hours in order to cure the epoxy. The assembly was allowed to cool to room temperature before performing the adhesion test. The test unit pulls the stud with a steadily increasing force until it breaks off the sample. For these measurements, a test was considered valid only if the HFCVD film covered by the stud was completely removed, exposing the silicon wafer surface. Six tests were run on each sample (each wafer was

divided into six pieces, with each piece tested separately) to obtain statistically significant values.

Saline soak testing and optical microscopy were performed under the supervision of Dr. David Edell at Innersea Technology. For this analysis, six “fluorocarbon-rich” films were deposited onto ½-inch diameter silicon wafers. The thickness of these films was approximately 13 μm. Test assemblies were prepared as follows. A ¼” inner diameter o-ring was first glued onto the test surface with silicone adhesive (MED4-4220) to define a test area. A silicone insulated wire (28 AWG, Bay Associates) used as a lead to external testing equipment was then connected onto backside of the test sample with Ni epoxy (10HTN, Master Bond Corporation). The partial assembly sample was then placed in a Teflon mold with the o-ring facing down, filled with silicone MED4-4220, and cured at 125 °C for 3 hours. The assemblies were then cooled and placed into glass tubes filled with saline solution. The test was performed with the saline at 37 °C by applying a DC bias on the sample, sweeping between –5 and +5 V. The resistivity of the sample was measured during each cycle. The duration of each cycle was approximately 72 hours. The soak test assembly is shown schematically in Figure A.1.

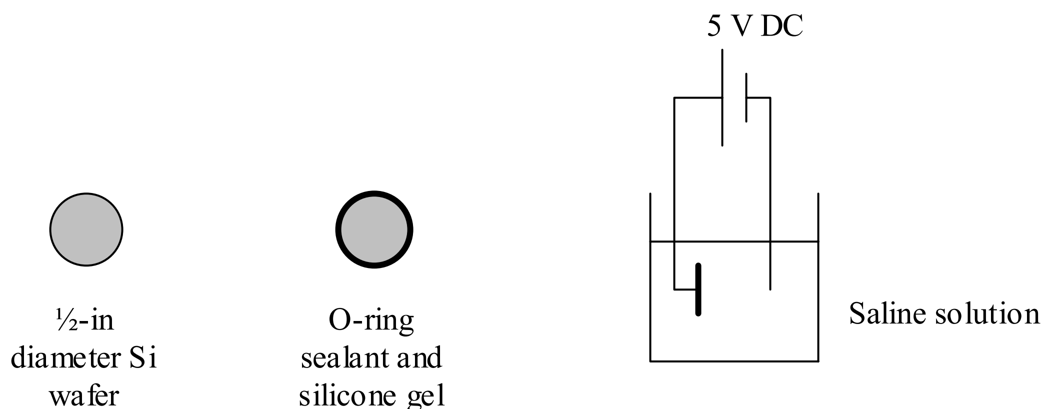

Figure A.1 Schematic diagram of soak test assembly.

A.3 Results and Discussion

Adhesion Tests. Table A.1 shows the adhesion test results for homopolymeric fluorocarbon and organosilicon films as well as the fluorocarbon-organosilicon copolymer. The presence of siloxane groups in the films greatly improves adhesion to silicon because these groups are capable of forming covalent bonds (Si-O-Si linkages) with the native oxide on the silicon surface.[4] The adhesion of the copolymer films to silicon is thus considerably better than that of fluorocarbon films. Furthermore, by varying the chemical composition of these films, their adhesion can be made better than that of organosilicon films.

This improvement in adhesion can be explained by considering the chemical structure of the organosilicon and copolymer films. Organosilicon films deposited from D_3 primarily consist of siloxane ring structures that are linked together in a network by Si-Si bonds.[5] Fluorocarbon-organosilicon films deposited from V_3D_3 and PFOSF at a low filament temperature consist of linear polymer chains with carbon backbones and siloxane ring

pendant groups.[2] Since the silicon atoms in the copolymer do not participate in backbone bonds, they would be available to form covalent bonds with the silicon substrate to a greater extent than silicon atoms in pure organosilicon films.

Table A.1 Adhesion test results for HFCVD films.

film type	adhesion (× 1000 psi)	comment
fluorocarbon	0.00	
fluorocarbon-organosilicon copolymer	0.30 ± 0.02	fluorocarbon-rich
	0.73 ± 0.03	organosilicon-rich
organosilicon	0.53 ± 0.06	

Saline Soak Tests and Optical Microscopy. Resistivity measurements from saline soak tests performed on six copolymer films are given in Table A.2. Resistivity values between 10^{12} and 10^{13} Ω-cm indicate good insulation. Smaller values indicate failure of the insulation. Of the six samples tested, only one sample retained good electrical insulation properties over the duration of 4 cycles (or 12 days). All of the other samples suffered failure during or shortly after the first cycle. Optical microscopy was performed on the samples in order to determine the cause of failure. Images of a film before and after soak testing are shown in Figure A.2.

Table A.2 Resistivity measurements from saline soak tests.

sample	1st cycle (Ω-cm)	2nd cycle (Ω-cm)	3rd cycle (Ω-cm)	4th cycle (Ω-cm)
A	2.07×10^{12}	2.13×10^{12}	4.09×10^{12}	5.43×10^{12}
B	6.60×10^{8}	1.14×10^{9}	5.38×10^{8}	1.04×10^{9}
C	9.92×10^{8}	3.59×10^{9}	1.19×10^{9}	4.97×10^{8}
D	1.13×10^{12}	1.54×10^{9}	3.97×10^{8}	6.28×10^{8}
E	1.09×10^{9}	1.85×10^{9}	--	--
F	1.52×10^{9}	-4.16×10^{9}	--	--

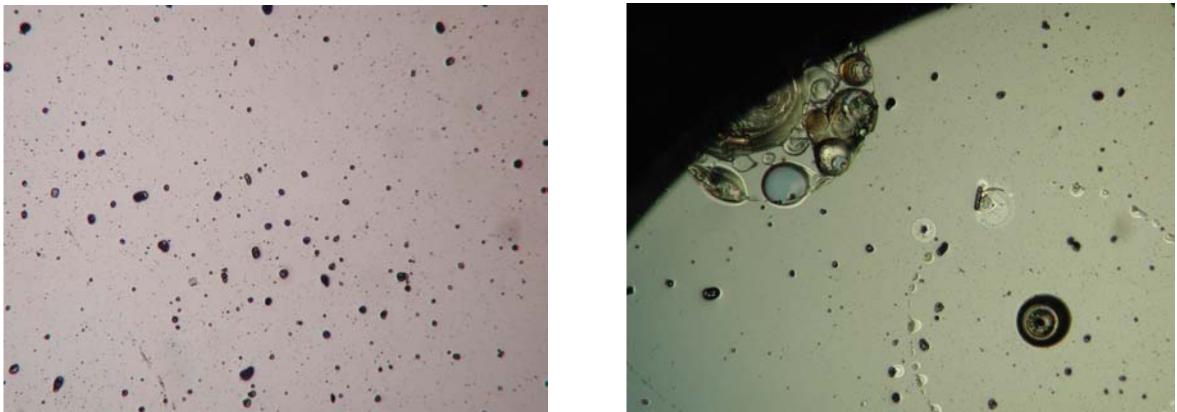

Figure A.2 Optical micrographs of a fluorocarbon-organosilicon copolymer film before (left) and after (right) saline soak testing. The surface of the film is covered with particles which appear to suffer corrosion upon immersion in saline.

The optical micrographs indicate that the surface of the copolymer films is covered by particles, which appear to undergo corrosion when the films are immersed in saline. This observation suggests that the particles have trace amounts of metal in them, most likely

incorporated from the filament, and points to the particles as the primary cause of the electrical failure. The formation of these particles is probably a consequence of flow patterns within the CVD chamber. If there are areas of recirculation, large polymer fragments could be produced in the gas phase before falling onto the substrate surface. The difference in behavior between the six samples (which were produced in the same HFCVD experiment) is probably due to different amounts of particulate matter present on the film surface.

A.4 Conclusions

Fluorocarbon-organosilicon copolymer films produced by HFCVD adhere well to silicon substrates. The strength of adhesion can be tuned by varying the composition of the films. Saline soak testing indicates that these films cannot perform well as insulators. This is most likely due to the presence of particulate matter present on the films surface. The particles may contain trace amounts of metal from the filament, which causes insulation failure and corrosion upon immersion in saline.

A.5 References

1. Murthy, S. K., Olsen, B. D. and Gleason, K. K. *J. Appl. Polym. Sci.*, (2003); submitted.
2. Murthy, S. K., Olsen, B. D. and Gleason, K. K. *Langmuir* **18**, 6424 (2002).
3. Murthy, S. K. and Gleason, K. K. *Macromolecules* **35**, 1967 (2002).
4. Wrobel, A. M. and Wertheimer, M. R. in *Plasma Deposition, Treatment, and Etching of Polymers* (eds. d'Agostino, R.) 163 (Academic Press, San Diego, 1990).
5. Pryce Lewis, H. G., Casserly, T. B. and Gleason, K. K. *J. Electrochem. Soc.* **148** (12), F212 (2001).